*Physiol Genomics* 23: 132–149, 2005.
First published July 20, 2005; doi:10.1152/physiolgenomics.00141.2004.

# Global transcriptional characterization of SP and MP cells from the myogenic C2C12 cell line: effect of FGF6

**Charles Decraene,[1] Rachid Benchaouir,[2] Marie-Agnes Dillies,[1] David Israeli,[2] Sylvie Bortoli,[1] Christelle Rochon,[1] Philippe Rameau,[2] Amandine Pitaval,[1] Diana Tronik-Le Roux,[1] Olivier Danos,[2] Xavier Gidrol,[1] Luis Garcia,[2] and Geneviève Piétu[1]**

[1]*Commissariat à l'Energie Atomique, Service de Génomique Fonctionnelle, and*
[2]*Genethon, Centre National de la Recherche Scientifique UMR 8115, Evry, France*

Submitted 15 June 2004; accepted in final form 14 July 2005

**Decraene, Charles, Rachid Benchaouir, Marie-Agnes Dillies, David Israeli, Sylvie Bortoli, Christelle Rochon, Philippe Rameau, Amandine Pitaval, Diana Tronik-Le Roux, Olivier Danos, Xavier Gidrol, Luis Garcia, and Geneviève Piétu.** Global transcriptional characterization of SP and MP cells from the myogenic C2C12 cell line: effect of FGF6. *Physiol Genomics* 23: 132–149, 2005. First published July 20, 2005; doi:10.1152/physiolgenomics.00141.2004.—With the use of Hoechst staining techniques, we have previously shown that the C2C12 myogenic cell line contains a side population (SP) that is largely increased in the presence of fibroblast growth factor 6 (FGF6). Here, we compared transcriptional profiles from SP and main population (MP) cells from either C2C12 or FGF6-expressing C2C12. Expression profiles of SPs show that these cells are less differentiated than MPs and display some similarities to stem cells. Moreover, principal component analysis made it possible to distinguish specific contributions of either FGF6 or differentiation effects on gene expression profiles. This demonstrated that FGF6-expanded SPs were similar to parental C2C12-derived SPs. Conversely, FGF6-treated MPs differed from parental MPs and were more related to SP cells. These results show that FGF6 pushed committed myogenic cells toward a more immature phenotype resulting in the accumulation of cells with a SP phenotype. We propose that FGF6 conditioning could provide a way to expand the pool of immature cells by myoblast dedifferentiation.

muscle; fibroblast growth factor 6; stem cell; microarray; principal component analysis

STEM CELLS have been identified in many adult tissues that undergo extensive cell replacement due to physiological turnover or injury. Until recently, these tissue-specific stem cells (SCs) have been considered monopotential, meaning they can give rise to cells contributing to homeostasis of the parental tissue, with little or no transdifferentiation occurring naturally. This accepted opinion has been reconsidered in the light of recent studies showing that hematopoietic SCs could participate in angiogenesis and muscle and hepatic regeneration as well as in the formation of central nervous system cell types (1, 13, 14, 25, 33, 44, 45). Conversely, it has been reported that blood cells could derive from SCs originating from different tissues (2, 26). Therefore, the bulk of information from the literature has suggested that SC populations display an "apparent" plasticity or versatility giving them the capability to differentiate into a range of distinct mature cells probably depending on the dominant effect of the local environment (for reviews, see Refs. 35 and 40). However, this hypothesis is challenged by recent findings showing that SCs used in these paradigms consisted of a mixture of SC from various origins (27, 32). In addition, it has been shown that these cells could also fuse with committed cells, thus indicating that transdifferentiation was not necessarily required to explain the plasticity of the SCs studied (49).

The rarity of these cells and the absence of specific markers have made the search for pure SC populations a challenge during the past years. Most of the studies have focused on the characterization of SCs using various well-known hematopoietic cell surface markers. The main limit of this approach is that purified cells consist of a mixture of cells from different lineages, which may share common surface markers. A way to purify the most immature cells from an adult tissue without prejudging their immunophenotypic characteristics is to use their properties to exclude vital dyes due to the fact that they highly express multidrug/ATP-binding cassette transporters (7, 52). As a result, SCs are only slightly stained in the presence of Hoechst 33342 and were collected using fluorescence-activated cell sorting (FACS) as a side population (SP) consisting of about 0.1–0.5% of total cells. Conversely, the more mature cells, forming the main population (MP), displayed low Hoechst excluding properties and thus were brightly stained. This technique was originally used to sort hematopoietic SCs with high repopulating activity when they were injected into lethally irradiated animals (17, 18, 46).

SP cells have been sorted from many tissues including skeletal muscle (20). However, immunophenotyping of the cells accumulated in these tissue-specific SP fractions showed a number of variations as well as a certain heterogeneity (3). Because skeletal muscle contains several types of cells (i.e., muscle, connective tissue, blood vessels, nerves, etc.), isolation of the most immature myogenic cells cannot be achieved by this method alone because the muscle-derived SP fraction would potentially consist of a mixture of putative SCs with varied differentiation properties. As an example, it has been shown that SP cells isolated from muscle biopsies may be either positive or negative for CD45 expression. All muscle-derived hematopoietic progenitor and in vivo bone marrow reconstitution activity is derived from CD45-positive cells (3). In addition, muscle-derived CD45-positive cells purified from uninjured muscle are uniformly nonmyogenic in vitro and do not form muscle efficiently in vivo compared with CD45-negative cells (3). More recently, it has been observed that CD45-positive cells purified from regenerating muscle readily gave rise to myoblasts (39). These results underline the high

Article published online before print. See web site for date of publication (http://physiolgenomics.physiology.org).

Address for reprint requests and other correspondence: G. Piétu, CECS/I-STEM, Batiment Généthon, 1 rue de l'Internationale, 91000 Evry, France (e-mail: gpietu@istem.genethon.fr).

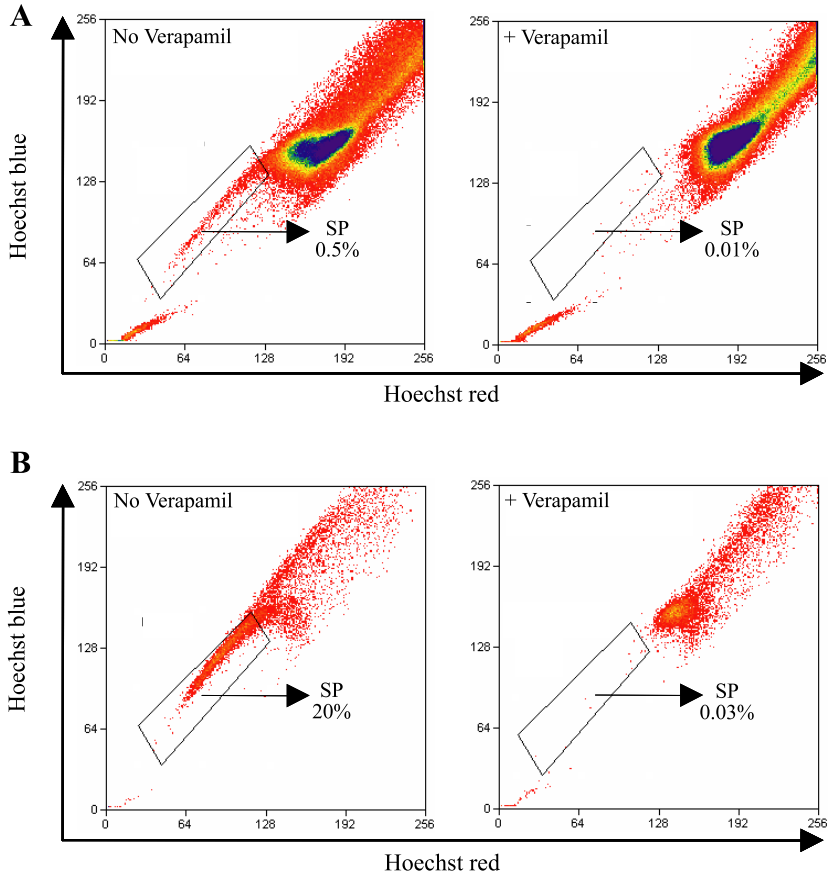


Fig. 1. Cell sorting analysis of C2C12 cells (*A*) or FGF6-transduced C2C12 cells (C2CF6 cells; *B*) after Hoechst 33342 treatment. The Hoechst diagrams were obtained after two preliminary cytometric selections: *1*) the morphological gate [*f* (forward scatter) = side scatter] was restricted around the side population (SP) region and *2*) inside the mortality diagram [*f* (forward scatter) = propidium iodide], dead cells were excluded because of their capacity to be marked by propidium iodide (data not shown).

complexity of the biology of the muscular SC and the difficulty to isolate cell populations using solely the expression of known expressed membrane markers.

A way to gain insight the molecular characterization of true muscle SP cells is to use a pure source of myogenic cells such as the C2C12 cell line. We established that the C2C12 cell line contained a subset of SP cells that consisted in quiescent cells sharing common features with regular SCs (5). Like muscle-derived SP cells and/or cell populations obtained by serial preplating or from disaggregated primary muscle, C2C12-derived SP cells exhibited reduced adhesion to plastic relative to fully committed myoblasts and required a longer time to recover myotube-forming capacities, features that are currently accepted as being those of early muscle precursor cells. C2C12-derived SP cells are CD34 and lymphocyte antigen 6 complex, locus A (*Sca1*)-positive and express ATP-binding cassette, subfamily B (MDR/TAP), member 1a (*mdr1a*). These cells are also myoblast determination protein (MyoD) low/− and resemble "dormant" cells because they are in the $G_0/G_1$ phase. In a recent study, Kondo et al. (29) also demonstrated that SP cells are present in a cell line, the malignant C6 glioma cell line, suggesting that the presence of a SP population in the myogenic C2C12 cell line is not a unique feature.

We used this model to investigate the possibility of expanding this fraction by using appropriate tissue culture conditions. Specifically, we (23) showed in a previous study that fibroblast growth factor 6 (FGF6) increases the C2C12-derived SP fraction by around 50 times. To ensure that such an increase was not due to insufficient dye staining, SP analysis was performed using a range of Hoechst concentrations. This work also showed that FGF6 selectively upregulates the *mdr1a* gene (but not the *mdr1b* gene) and suggested a role for FGF6 in the maintenance of a reserve pool of progenitor cells in skeletal muscle.

Here, our goal was to initiate the characterization of the genetic program in SP and MP cells sorted from either C2C12 or FGF6-expressing C2C12 (C2CF6). This would first give us a standard baseline for primary muscle SCs and also make it possible to determine whether SP cells obtained in the presence of FGF6 are equivalent to canonical SPs.

Recent publications (24, 41) show that microarray technology is an important tool for the characterization of SCs. Previously, a large number of cells was required to perform such analysis, essentially excluding the use of the microarray technology for cells that are too infrequent in vivo, as it is the case for SCs. Here, we used the in vitro transcription RNA amplification procedure first described by Van Gelder et al. (48), which allowed us to perform global expression profiling of genes in SP and MP populations from C2C12 cells transduced or not by FGF6 using $<$100,000 cells in each sorted fraction.

With the use of microarray analysis, we characterized the transcriptome of both SP and MP cells purified from C2C12 (S2 and M2 cells) or C2CF6 (S6 and M6 cells). The differential analysis of expression patterns allowed us to dissociate the effects of FGF6 from that of differentiation and to define the transcriptional signature of these SP cells.

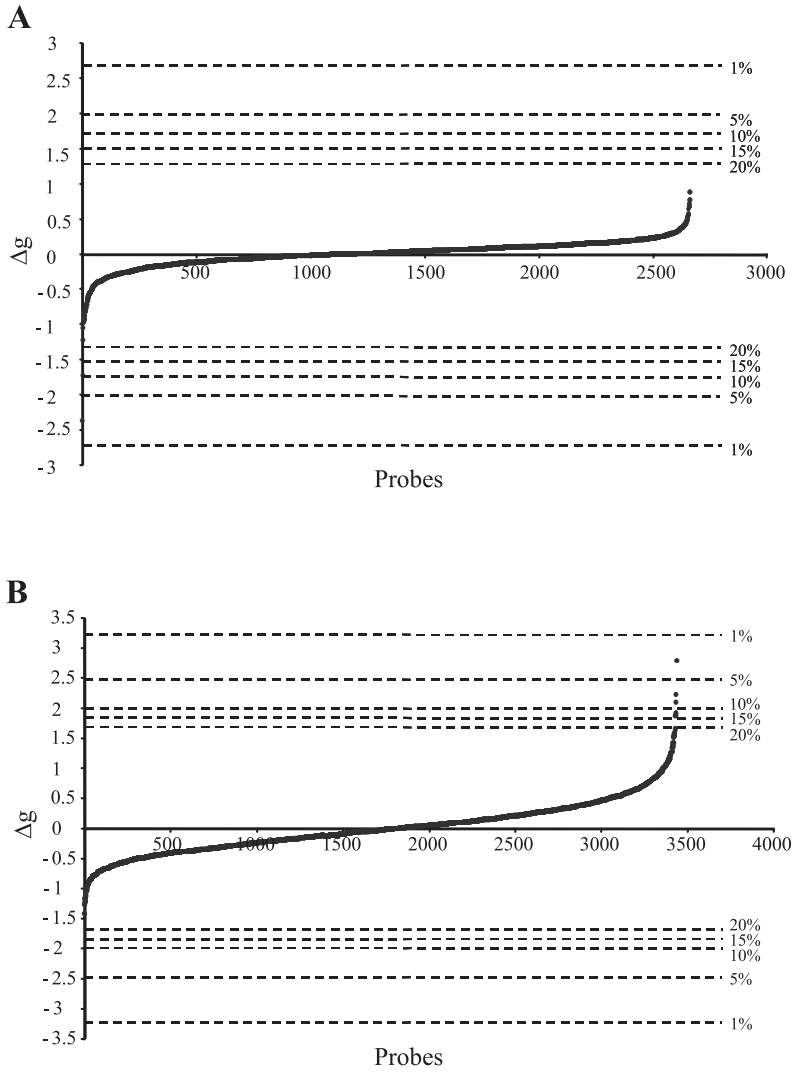


Fig. 2. Differential scores ($\Delta g$) obtained for all the 7,690 probes sorted in the ascending order using the same identical target. *A*: cDNA target derived from total RNA. *B*: cDNA target derived from amplified RNA. Horizontal lines above and below the plot correspond to the upper and lower 1, 5, 10, 15, and 20% type I error rate thresholds.

## MATERIALS AND METHODS

### *Cell Cultures and RNA Preparation*

C2C12, a subclone of the C2 mouse myoblast cell line (6, 50), was obtained from the American Type Culture Collection. The C2C12 cell line retrovirally transduced by a murine leukemia virus-derived vector recombinant for a *bis*-cistronic construction consisting of a murine FGF6 and green fluorescent protein (GFP) cDNA separated by internal ribosome entry site (IRES) as previously described (23) was named C2CF6. Cell cultures, Hoechst staining, and FACS analysis were performed as previously described (23). About 30,000–50,000 SP cells were obtained from each sorting starting with a total of $10 \times 10^6$ cells. Total RNA was extracted from the FACS-sorted cells using the Absolutely RNA Microprep Kit as described in the manufacturer's protocol (Stratagene). One microgram of total RNA from each sample was amplified using the MessageAmp Amplified RNA (aRNA) Kit (Ambion) according to the manufacturer's protocol. The integrity of total RNA and aRNA was verified using a Bioanalyzer (Agilent).

### *Production of DNA Microarrays*

DNA microarrays were generated using a collection of 7,200 probes. A total of 1,700 mouse cDNA clones (as bacterial colonies) was obtained from Research Genetics. Approximately 1,400 genes were represented in this set of clones (according to Unigene cluster comparison). All these clones are from Integrated Molecular Analysis of Genome and Their Expression libraries and have been sequence verified. The cDNA clone inserts were amplified using two primers complementary to flanking sequences in the cloning vector [M13(–21) and M13 REV]. A total of 2,200 PCR products was obtained using specific oligonucleotides based on a selection of genes chosen as responsive to keywords like stem cell, apoptosis, growth factors, transcription factors, etc. One thousand five hundred mouse cDNA clones were produced from a subtracted library (mdx muscle/normal muscle) and 1,800 rat cDNA clones from another subtracted library (atrophied muscle/normal muscle). The 7,200 PCR products were analyzed by electrophoresis on an agarose gel for quality control and quantitation and then ethanol precipitated. Control probes were added at least in duplicate, including positive controls (GAPDH, actin, and tubulin) and negative controls (genes of plant, plasmid DNA, and TE/DMSO). Finally, a total of 7,690 probes was spotted on the slide. Microarrays were prepared by printing PCR-amplified probes, arrayed in 384-well microtiter plates, suspended in a spotting buffer composed of 50% DMSO and TE on AminoSilane slides (CMT GAPS II, Corning) with a robot Microgrid II (BioRobotics) at a density of 1,000 cells/cm$^2$ under a controlled atmosphere.

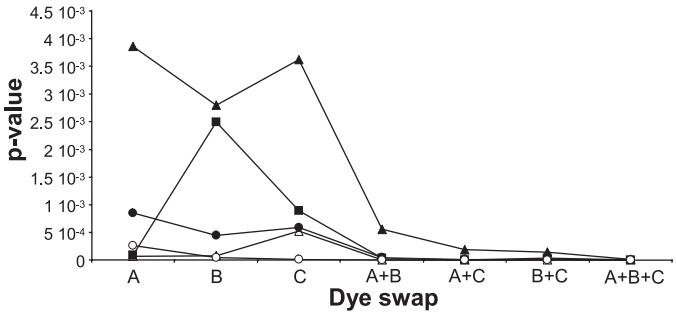


Fig. 3. Evolution of the *P* value for 5 genes in as a function of the number of dye swaps (*A–C*) involved in the experiment.

*Target Preparation and Array Hybridization*

For each target preparation, 1 μg of aRNA was reverse transcribed using SuperscriptTM II reverse transcriptase (Life Technologies) in the presence of random hexamers and an amino-modified nucleotide (amino allyl dUTP). Amino-modified cDNAs were purified through a Microcon Centricon 30 microconcentrator (Amicon) and ethanol precipitated. In a second step, monofunctional forms of Cy3 and Cy5 dyes (Amersham) were coupled with the purified amino-modified cDNAs. Unincorporated fluorescent molecules and salts were removed through the Microcon Centricon 30. Labeled cDNA was mixed with 10 μg poly(A) RNA (Boehringer), 10 μg tRNA (Life Technologies), and 10 μg mouse Cot1 DNA (Life Technologies). Each slide was rehydrated over boiling water and quickly heated on a hot plate, and the probes were ultraviolet light cross-linked in a Stratalinker at 254 nm/250 mJ. The slides were prehybridized in 5× SSC-0.1% SDS-1% BSA for 30 min at 50°C. Purified labeled targets were resuspended in 40 μl of hybridization solution (70% formamide-3.6× Dehnardt-0.7% SDS-8.6× saline-sodium phosphate-EDTA) and heated at 95°C for denaturation. The labeled targets were applied to prehybridized slides and covered with a 60 × 22-mm polyethylene coverslip (Sigma). The hybridization was performed at 42°C overnight. Washings were performed at room temperature for 15 min in 0.1× SSC-0.1% SDS and for 2 × 15 min in 0.1× SCC.

*Data Processing*

After hybridization and washing, fluorescent signals were acquired by scanning each slide using the ScanArray 5000 scanner (Packard). A separate image was captured for each of the two fluorophores used. The resolution of the scan was 10 μm/pixel on a gray scale. The .tiff images resulting from the scan were imported into image-analysis GenePix Pro 4.0 software (Axon) to quantitate the signal for each spot. Spots with obvious blemishes were flagged. Genes with null intensity values and low mean intensity were also annotated with a specific flag. All the array elements (flagged or not flagged) were included in the statistical analysis, but flagged elements were excluded from the list of validated differentially expressed genes.

*Statistical Analysis of Experimental Data*

*ANOVA.* Standard ANOVA was performed on the logarithm of raw gene expression data without prior background subtraction. Four main factors were included in the model as well as four two-order interaction factors, as proposed in Ref. 28. The model equation is given by *Eq. 1*:

$$y_{ijkl} = (A)_i + (D)_j + (V)_k + (G)_l + (AD)_{ij} + (AG)_{il} + (DG)_{jl} + (VG)_{kl} + \varepsilon_{ijkl} \quad (1)$$

where *A*, *D*, *V*, and *G* denote, respectively, the array, dye, variety (or biological condition), and gene effects, $y_{ijkl}$ is the measured intensity values for *gene l* spotted on the *i*th array (on which biological *condition k* was labeled with *dye j*), and $\epsilon_{ijkl}$ is the error term. A lowess (local linear regression) correction (51) was first applied independently on each array for which a nonlinear relationship between the mean spot log intensity and the difference between spot log intensities [M-A plot (12)] was observed. The first three main effects were then corrected by subtracting, for each factor modality, the amplitude of the difference between the modality mean level and the global mean intensity of the experiment. *Equation 2* shows as an example the correction equation for the array effect:

$$y'_{ijkl} = y_{ijkl} - (m_i - m),\ i = 1, \ldots N_A \quad (2)$$

where $N_A$ is the number of arrays included in the experiment, $y'_{ijkl}$ denotes the corrected $y_{ijkl}$ value, and *m* is the global mean intensity of the experiment.

Once these corrections had been performed, the corresponding effects were suppressed from the ANOVA model. The possibly remaining factors that could not be corrected were then accounted for in the model residues. The resulting model was then of the following form [*Eq. 3* (43)]:

$$y_{kl} = (G)_l + (VG)_{kl} + \varepsilon_{kl} \quad (3)$$

where $(G)_l$ is the only main effect that cannot be corrected because of the small number of intensity values per gene and $(VG)_{kl}$ is the variability of interest, because it is significant for genes that are differentially expressed.

*Selection of differentially expressed genes.* Differentially expressed genes were then identified using a classical parametric hypothesis test of mean comparison. A differential score $\Delta g$ was computed for each gene as the difference between the mean intensity values in the two biological conditions that are compared (*Eq. 4*):

$$\Delta_g = m_{1g} - m_{2g} \quad (4)$$

Let us assume that the measured intensity values for all the genes follow a normal distribution with mean $m_g$ and the same variance $\sigma^2$

Table 1. *Distribution of genes after 2-by-2 statistical analysis according to their function identified in the Gene Ontology database*

| | M2M6U | M2M6D | M2S2U | M2S2D | M2S6U | M2S6D | M6S2U | M6S2D | M6S6U | M6S6D | S2S6U | S2S6D |
|---|---|---|---|---|---|---|---|---|---|---|---|---|
| RNA synthesis | 2 | 0 | 1 | 2 | 3 | 2 | 1 | 3 | 1 | 1 | 1 | 2 |
| Protein synthesis | 0 | 0 | 0 | 0 | 0 | 0 | 0 | 1 | 0 | 0 | 0 | 0 |
| Metabolism | 8 | 6 | 3 | 1 | 4 | 8 | 5 | 6 | 5 | 6 | 2 | 3 |
| Cell shape | 9 | 0 | 8 | 0 | 9 | 1 | 0 | 2 | 1 | 1 | 2 | 1 |
| Cell signaling | 4 | 2 | 2 | 1 | 4 | 7 | 3 | 2 | 5 | 1 | 4 | 2 |
| Cell division | 2 | 1 | 2 | 3 | 4 | 4 | 1 | 2 | 4 | 2 | 4 | 2 |
| Cell defense | 0 | 1 | 1 | 2 | 0 | 0 | 0 | 0 | 2 | 2 | 1 | 0 |
| Miscellaneous | 1 | 1 | 2 | 3 | 3 | 4 | 3 | 2 | 1 | 1 | 3 | 3 |

For each comparison, in each column; *XY*U, is upregulation in *cell fraction X* compared with cell fraction *Y* and *XY*D, downregulation in *cell fraction X* compared with *cell fraction* Y, where *X* and *Y* are the M2, M6, S2, or S6 cell fractions.

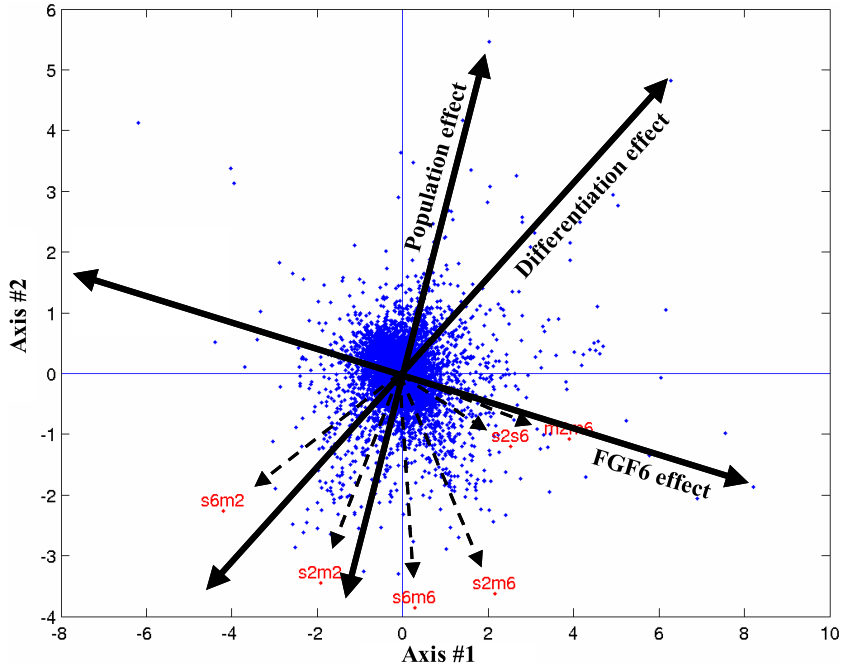


Fig. 4. Schematic representation of the principal component analysis. Dashed arrays are a graphical representation of the 6 variables (or experiments) on the first 2 principal components. They provide information about their contribution to the definition of these 2 axes. The percentage of variance explained by each axis is given. Thus the first 2 axes explain almost 70% of the total variance of the data set, which means that the graphical representation of the projected data set is quite reliable. Solid arrays represent the directions of the main global effects. Hypotheses about the role of outlier genes can be deduced from their position with respect to these main arrays.

(hypothesis of homoscedasticity of genes). Then, $\Delta g$ follows a normal distribution with standard deviation $2 \times \sigma^2/N_A$. Under the null hypothesis of unaffected expression, $\Delta g$ is also of mean 0. So the hypothesis test is expressed as follows: test $H_0$: $\Delta g = 0$ vs. $H_1$: $\Delta g \neq 0$, where $H_0$ is the null hypothesis and $H_1$ is the alternative hypothesis. $\sigma^2$ can be estimated as the variance of the residuals in the ANOVA model given in (*Eq. 3*). Because it is computed over all the measured intensity values, it can be considered as a robust estimate. Under the hypothesis of homoscedasticity of genes, differentially expressed genes are those for which the null hypothesis is rejected with a given error risk $\alpha$.

Let $X$ be a normal random variable with mean 0 and standard deviation $\sigma$ and $a$ be a real value so that the probability that $|X|$ is greater than $a$, $P(|X| > a) = \alpha$. Then, *gene g* is considered as differentially expressed if

$$|\Delta g| > a\sigma\sqrt{\frac{2}{N_A}}$$

Note that this threshold value is inversely proportional to the square root of the number of dye swaps involved in the experiment. Thus, as the number of replicates increases, the decision threshold decreases, resulting in a larger number of genes that are found to be significantly differentially expressed. The assumption that all the genes exhibit the same intensity variance is, of course, not valid. It is valid only for genes that fit the proposed ANOVA model. Genes that do not fit the model can be detected by computing the residual variance independently for each gene and comparing the resulting distribution to a $\chi^2$-distribution with $(N_A - 1)$ degrees of freedom. For genes that passed the first hypothesis test of differential expression but do not fit the model, a separate variance analysis can be performed, but the power of the test is then greatly reduced. These genes are finally considered as differentially expressed if the biological condition effect is significant (42).

*Global analysis with principal component analysis.* Principal component analysis (PCA) is a descriptive multivariate data analysis method. It enables exploration of the structure of large data sets in which data points are described by a large number of variables that prevents visualizing it. PCA takes advantage of the correlation that exists between the variables. It provides a projection of the data set in a new space of reduced size that allows visualization in a two-dimensional space while minimizing the loss of information. The axes of this new space are called principal components. They are defined as linear combinations of the original variables. Two graphical representations result from a PCA: the "data set" representation and the "variables" one.

In the first type of graph, the data points are plotted in the new space. A restriction to the first two principal components makes it possible to visualize the structure of the data set as well the proximity between data points. Thus data points that appear to be close in this two-dimensional space may be similar with respect to the original variables that were chosen to describe them, given that the projected data set is close to the original one. Outliers are data points whose values for the original variables are far from the mean values exhibited by the whole data set.

The second type of graph shows the correlations between the original variables and principal components. It points out the variables that influence at most the structure of the data set. Both representations provide a complementary view of the data set. They may be superimposed on a single graph.

Most computations for the data analysis were carried out using R software (22) except for global analyses, which were performed using either Matlab software (Mathworks; Natick, MA) or SAS software (SAS Institute; Cary, NC). The microarray dataset used for this analysis is described and available from GEO (GSE1436 and GSM241086–GSM24142).

*Real-time quantitative RT-PCR analysis.* RNA samples prepared from SP and MP cells purified from C2C12 (S2 and M2 cells) or C2CF6 (S6 and M6 cells) were analyzed by RT-PCR using the One-Step RT-PCR Kit (Qiagen) with 10 ng RNA. The incorporation of SYBR green dye into PCR products was monitored in real time with an ABI PRISM 7700 sequence detection system (PE Applied Biosystems). The efficiency of the amplification was determined for each pair of primers by comparison with a standard curve generated with serially diluted cDNA. Target genes were quantified relative to a reference gene (18S) using the mathematical model described by Pfaffl (37). All PCRs were performed in triplicate. Primers were as follows: $\alpha_1$-actin (*Acta1*), forward 5′-GTGAGATTGTGCGCGACATC-3′ and reverse 5′-GGCAACGGAAACGCTCATT-3′; IGF

Table 2. *Upregulated genes implicated in the FGF6 effect identified using global ANOVA and differential analysis*

| Differential of Expression | Gene Symbol | GenBank Accession No. | Unigene | Product | Redundancy |
|---|---|---|---|---|---|
| | | | | *RNA synthesis* | |
| 3.58 | *Rmga1* | AA153319 | Mm.4438 | High-mobility group AT-hook 1 | 1 |
| 2.63 | *Nfe2l2* | AA163371 | Mm.1025 | Nuclear factor, erythroid-derived 2, like 2 | 1 |
| 1.87 | *Nfatc2* | U02079 | Mm.116802 | Nuclear factor of activated T cells, cyloplasmic 2 | 1 |
| 1.84 | *Skiv2l* | AA097885 | Mm.18845 | Superkiller viralicidic activity 2-like (*S. cerevisiae*) | 1 |
| 1.74 | *Aes* | AI326366 | Mm.2626 | Amino-terminal enhancer of split | 1 |
| 1.73 | *Atf4* | AB012277 | Mm.641 | Activating transcription factor 4 | 1 |
| 1.55 | *gfi2* | | | GLI-Kruppel family member GLI2 | 1 |
| 1.51 | *Snrpe* | X65704 | Mm.27669 | Small nuclear ribonucleoprotein E | 1 |
| 1.49 | *Tgif* | AA060371 | Mm.8155 | TG interacting factor | 1 |
| 1.42 | *Pparg* | AI893887 | Mm.3020 | Peroxisome proliferator-activated receptor-γ | 1 |
| 1.41 | *Polr2c* | D83999 | Mm.2186 | Polymerase (RNA) II (DNA directed) polypeptide C | 1 |
| | | | | *Protein synthesis* | |
| 1.67 | *Ubb* | X51703 | Mm.235 | Ubiquitin B | 1 |
| 1.64 | *Rpl12* | L04280 | Mm.70127 | Ribosomal protein L12 | 1 |
| 1.50 | *Rpl30* | AA166608 | Mm.3487 | Ribosomal protein L30 | 1 |
| | | | | *Metabolism* | |
| 4.80 | *Slpi* | U94341 | Mm.1395 | Secretory leukocyte protease inhibitor | 2 |
| 4.35 | *Hmgcs2* | AA105375 | Mm.10633 | 3-Hydroxy-3-methylglutaryl-CoA synthase 2 | 1 |
| 3.99 | *Upp* | D44464 | Mm.4610 | Uddine phosphorylase | 1 |
| 3.88 | *Slc6a9* | AI323390 | Mm.2834 | Solute carrier family 6, member 9 | 1 |
| 3.61 | *ABCA8* | NM_007168 | Hs.38095 | ATP-binding cassette, subfamily A, member 8 | 1 |
| 3.01 | *Hbb-b1* | AI324016 | Mm.30266 | Hemoglobin, β-adult major chain | 1 |
| 2.68 | *Slc20a1* | AI385598 | Mm.16757 | Solute carrier family 20, member 1 | 1 |
| 2.46 | *Nt5e* | AA138262 | Mm.56948 | 5′-Nucleotidase, ecto | 1 |
| 2.45 | *Ctsf* | AF136280 | Mm.29561 | Cathepsin F | 1 |
| 2.37 | *Prdx6* | AF197951 | Mm.193042 | Peroxiredoxin 6 | 2 |
| 2.36 | *Slc3a2* | AA162505 | Mm.4114 | Solute carrier family 3, member 2 | 1 |
| 2.35 | *Cslb* | AI324888 | Mm.6095 | Cystatin B | 1 |
| 2.26 | *Pam* | AI323101 | Mm.5121 | Peptidylglycine α-amidating monooxygenase | 1 |
| 2.25 | *Pycs* | AI894364 | Mm.29751 | Pyrroline-5-carboxylate synthetase | 1 |
| 2.23 | *Fxyd5* | U72680 | Mm.1870 | FXYD domain-containing ion transport regulator 5 | 1 |
| 2.16 | *Ugt1a1* | AA137865 | Mm.42472 | UDP-glucuronosyltransferase 1 family, member 1 | 1 |
| 2.04 | *Prdx4* | AA170690 | Mm.19127 | Peroxiredoxin 4 | 1 |
| 1.96 | *Ech1* | AF030343 | Mm.2112 | Enoyl CoA hydratase 1, peroxisomal | 1 |
| 1.91 | *Mthfd2* | AA011762 | Mm.443 | Methylenetetrahydrofolate dehydrogenase ($NAD^+$ dependent) | 1 |
| 1.84 | *Nars* | W33838 | Mm.29192 | Asparaginyl-tRNA synthetase | 1 |
| 1.72 | *Gaa* | W10979 | Mm.4793 | Glucosidase, α, acid | 1 |
| 1.72 | *Ndufa2* | AA162428 | Mm.29867 | NADH dehydrogenase (ubiquinone) 1-α, subcomplex, 2 | 1 |
| 1.70 | *Pitpn* | AI327361 | Mm.3128 | Phosphatidylinositol transfer protein | 1 |
| 1.68 | *Spr* | AA016369 | Mm.28393 | Sepiapterin reductase | 2 |
| 1.66 | *Tkt* | AA162373 | Mm.154387 | Transketotase | 1 |
| 1.65 | *Slc25a11* | AA154189 | Mm.28466 | Solute carrier family 25, member 11 | 1 |
| 1.62 | *Atpi* | AF002718 | Mm.2171 | ATPase inhibitor | 1 |
| 1.62 | *Crot* | AA107144 | Mm.28197 | Camitine *O*-octanoyltransferase | 1 |
| 1.61 | *Eno3* | X57747 | Mm.29994 | Enolase 3, β-muscle | 1 |
| 1.50 | *Mor2* | M29462 | Mm.3156 | Malate dehydrogenase, soluble | 2 |
| 1.48 | *Alox5ap* | AI893311 | Mm.19844 | Arachidonate 5-lipoxygenase-activating protein | 1 |
| 1.47 | *Cox7a3* | AF037371 | Mm.2151 | Cytochrome *c* oxidase, subunit VIIa 2 | 1 |
| 1.44 | *Prdx1* | AA170669 | Mm.30929 | Peroxiredoxin 1 | 1 |
| 1.44 | *Idh1* | AI325900 | Mm.9925 | Isocitrate dehydrogenase 1 ($NADP^+$), soluble | 1 |
| 1.44 | *Umps* | M29395 | Mm.13145 | Uridine monophosphate synthetase | 1 |
| 1.43 | *Abcb4* | AA434959 | Mm.14172 | ATP-binding cassette, subfamily B, member 4 | 1 |
| 1.42 | *Siat1* | AA059687 | Mm.226696 | Sialyltransferase 1 | 1 |
| 1.42 | *Cyp2e1* | AA163172 | Mm.21758 | Cytochrome *P*-450, family 2, subfamily e, polypeptide 1 | 1 |
| 1.42 | *Ftl1* | J04716 | Mm.7500 | Ferritin light chain 1 | 1 |
| | | | | *Cell shape* | |
| 2.18 | *Tnnt3* | L49470 | Mm.14546 | Troponin T3, skeletal, fast | 1 |
| 2.11 | *Anxa1* | AA170204 | Mm.14860 | Annexin $A_1$ | 2 |
| 2.05 | *Anxa11* | AA031147 | Mm.1427 | Annexin $A_{11}$ | 1 |
| 1.74 | *Anxa7* | L13129 | Mm.20794 | Annexin $A_7$ | 1 |
| 1.52 | *Add2* | AA051689 | Mm.104155 | Adducin 2 (β) | 1 |
| 1.47 | *Mglap* | D00613 | Mm.193459 | Matrix γ-carboxyglutamate protein | 1 |

*Continued*

Table 2. *continued*

| Differential of Expression | Gene Symbol | GenBank Accession No. | Unigene | Product | Redundancy |
|---|---|---|---|---|---|
| | | | | *Cell signaling* | |
| 4.51 | *Igfbp4* | AI894365 | Mm.22248 | IGF binding protein 4 | 1 |
| 4.07 | *Alcam* | U9503D | Mm.2877 | Activated leukocyte cell adhesion molecule | 1 |
| 3.00 | *Spp1* | A1325605 | Mm.321 | Secreted phosphoprotein 1 | 1 |
| 2.78 | *Dlgh3* | AA170453 | Mm.4615 | Discs, large homolog 3 (*Drosophila*) | 1 |
| 2.73 | *Dusp1* | AI325917 | Mm.2404 | Dual-specificity phosphatase 1 | 1 |
| 2.61 | *Igf2r* | U04710 | Mm.2938 | IGF 2 receptor | 1 |
| 2.35 | *Rab5c* | AA161814 | Mm.29829 | RAB5C, member of the RAS oncogene family | 1 |
| 2.08 | *Fgfr1* | AI326934 | Mm.3157 | FGF receptor 1 | 1 |
| 1.93 | *Rac3* | AI325868 | Mm.27318 | RAS-related C3 *botulinum* substrate 3 | 1 |
| 1.78 | *Fzd8* | AI385637 | Mm.25171 | Frizzled homolog 8 (*Drosophila*) | 1 |
| 1.75 | *Calm1* | AF178845 | Mm.34246 | Calmodulin 1 | 1 |
| 1.68 | *Il2rb* | M28052 | Mm.931 | Interleukin 2 receptor, β-chain | 1 |
| 1.66 | *Ptpn8* | AA124804 | Mm.395 | Protein tyrosine phosphatase, nonreceptor type B | 1 |
| 1.66 | *S100a10* | AA166385 | Mm.1 | S100 calcium-binding protein A10 (calpactin) | 1 |
| 1.61 | *Oprs1* | AF030198 | Mm.22745 | Oploid receptor, $\sigma_1$ | 1 |
| 1.60 | *Camk2d* | W30289 | Mm.34377 | Calcium/calmodulin-dependent protein kinase II, δ | 1 |
| 1.56 | *Chp-pending* | AI324070 | Mm.27065 | Calcium-binding protein P22 | 1 |
| 1.53 | *Gabarapl2* | AA154850 | Mm.30017 | GABAA receptor-associated protein-like 2 | 1 |
| 1.53 | *Neo1* | AI325842 | Mm.42249 | Neogenin | 1 |
| 1.52 | *Gnai2* | AI894344 | Mm.196464 | Guanine nucleotide binding protein, α-inhibiting 2 | 1 |
| 1.42 | *Rabac1* | AA123361 | Mm.22473 | Rab acceptor 1 (prenylated) | 1 |
| | | | | *Cell division* | |
| 7.88 | *MDM2* | | | Transformed mouse 3T3 cell double minute 2 | 1 |
| 2.95 | *ank* | AF001533 | Mm.142714 | Progressive ankylosis | 1 |
| 2.82 | *mertk* | AA125559 | Mm.4582 | C-mer protooncogene tyrosin kinase | 1 |
| 2.49 | *ler3* | AA122977 | Mm.25613 | Immediate-early response 3 | 1 |
| 2.08 | *PNQLARE* | AI326314 | Mm.202346 | CDK-related protein kinase PNQLARE | 1 |
| 2.04 | *Cenpa* | AF012709 | Mm.6579 | Centromere autoantigen A | 1 |
| 2.04 | *Evi2* | M34896 | Mm.3266 | Ecotropic viral integration site 2 | 1 |
| 1.84 | *Btg1* | AA163356 | Mm.16596 | β cell translocation gene 1, antiproliferative | 1 |
| 1.74 | *Rad9* | AA155443 | Mm.193035 | RAD9 homolog (*S. pombe*) | 1 |
| 1.74 | *Ccnb2* | X66032 | Mm.22592 | Cyclin $B_2$ | 1 |
| 1.73 | *Ret* | X67812 | Mm.57199 | *Ret* protooncogene | 1 |
| 1.72 | *Pcna* | A1385898 | Mm.7141 | Proliferating cell nuclear antigen | 2 |
| 1.64 | *CCRK* | AF035013 | Mm.202346 | CDK-related protein kinase PNQLARE | 1 |
| 1.64 | *Capns1* | AF058298 | Mm.6534 | Calpain, small subunit 1 | 1 |
| 1.59 | *Pold2* | Z72486 | Mm.35788 | Polymerase (DNA directed), $\delta_2$, regulatory subunit | 2 |
| 1.49 | *Bad* | AA237527 | Mm.4387 | Bcl-associated death promoter | 1 |
| 1.43 | *Ddx5* | AA120483 | Mm.19101 | Asp-Glu-Ata-AspHis box polypeptide 5 | 1 |
| 1.43 | *Bcl2a1a* | AI326167 | Mm.196731 | β cell leukemialymphoma 2-related protein A1a | 1 |
| | | | | *Cell defense* | |
| 2.13 | *H2-T23* | AA060835 | Mm.35016 | Histocompatibility 2, T region locus 23 | 1 |
| 2.04 | *Il3* | K01668 | Mm.983 | Interleukin 3 | 1 |
| 1.95 | *Pnkp* | AA162545 | Mm.29545 | Polynucleotide kinase 3′-phosphatase | 1 |
| 1.92 | *Gpx4* | DB7896 | Mm.2400 | Glutathione peroxidase 4 | 1 |
| 1.83 | *C1qb* | M36293 | Mm.2570 | Complement component 1, q subcomponent, β-polypeptide | 1 |
| 1.74 | Hsp70–2 | AI326309 | Mm.57245 | Heat shock protein 70–72 | 1 |
| 1.64 | *Gstz1* | AA139820 | Mm.29652 | Glutathione transferase $\zeta_1$ (maleylacetoacelate isomerase) | 1 |
| 1.60 | *Ktra7* | U10094 | Mm.193478 | Killer cell lectin-like receptor, subfamily A, member 7 | 1 |
| 1.59 | *Ccr6* | AB016031 | Mm.8007 | Chemokine (C-C motif) receptor 6 | 1 |
| 1.52 | *Gsto1* | U80819 | Mm.282 | Glutathione *S*-transferase-$\omega_1$ | 1 |
| 1.43 | *Fcer1g* | AA072722 | Mm.22673 | Fc receptor, IgE, high-affinity I, γ-polypeptide | 1 |
| 1.42 | *Psme1* | U60328 | Mm.830 | Proteasome (prosome, macropain) 28 subunit, α | 1 |
| | | | | *Miscellanous* | |
| 2.89 | *Sat* | L10244 | Mm.2734 | Spermidinespermine *N*1-acetyl transferase | 1 |
| 2.81 | *Gp38* | M73748 | Mm.2976 | Glycoprotein 38 | 2 |
| 2.75 | *Tm4sf1* | L15429 | Mm.856 | Transmembrane 4 superfamily, member 1 | 1 |
| 2.63 | *Sema5a* | AI385610 | Mm.24733 | Semaphorin 5A | 1 |
| 1.95 | *Myd116* | AA155095 | Mm.4048 | Myeloid differentiation primary response gene 116 | 1 |
| 1.94 | *Fth* | J03941 | Mm.1776 | Ferritin heavy chain | 1 |

*Continued*

Table 2. *continued*

| Differential of Expression | Gene Symbol | GenBank Accession No. | Unigene | Product | Redundancy |
|---|---|---|---|---|---|
| 1.93 | *Apobec1* | AA073652 | Mm.3333 | Apolipoprotein B editing complex 1 | 1 |
| 1.89 | *Lgals3* | X16834 | Mm.2970 | Lectin, galactose binding, soluble 3 | 1 |
| 1.82 | *Timm8b* | AA142731 | Mm.141867 | Translocase of inner mitochondrial membrane 8 homolog b (yeast) | 1 |
| 1.76 | *Hint* | U60001 | Mm.425 | Histidine triad nucleotide binding protein | 2 |
| 1.76 | *Dp1* | AA032729 | Mm.21251 | Deleted in polyposis 1 | 1 |
| 1.71 | *Nubp1* | AA152999 | Mm.29037 | Nucleotide binding protein 1 | 1 |
| 1.69 | *Tactile-pending* | AA154092 | Mm.29204 | T cell activation, increased late expression | 1 |
| 1.66 | *Sui1-rs1* | AA138667 | Mm.13886 | Suppressor of initiator codon mutations, related sequence 1 (*S. cerevisiae*) | 1 |
| 1.60 | *Lamp1* | M25244 | Mm.16716 | Lysosomal membrane glycoprotein 1 | 1 |
| 1.54 | *Urod* | AI893349 | Mm.22494 | Uroporphyrinogen decarboxylase | 1 |
| 1.52 | *Tctex1* | M25825 | Mm.1948 | t-complex testis expressed 1 | 1 |
| 1.50 | *Thbd* | AI385582 | Mm.24096 | Thrombomodulin | 1 |
| 1.50 | *Adfp* | M93275 | Mm.381 | Adipose differentiation-related protein | 1 |
| 1.50 | *Mcmd4* | AI325074 | Mm.1500 | Minichromosome maintenance deficient 4 homolog (*S. cerevisiae*) | 1 |
| 1.49 | *Tff3* | AI323301 | Mm.4641 | Trefoil factor 3, intestinal | 1 |
| 1.47 | *Bckdha* | AI323918 | Mm.25848 | Branched chain ketoacid dehydrogenase $E_1$, α-polypeptide | 1 |
| 1.47 | *Cd34* | AI893233 | Mm.29798 | CD34 antigen | 1 |
| 1.46 | *Ap3m1* | AA049853 | Mm.3256 | Adaptor-related protein complex 3, $\mu_1$-subunit | 1 |
| 1.43 | *Copz2* | AI327160 | Mm.22144 | Coatomer protein complex, subunit $\zeta_2$ | 1 |
| 1.43 | *DDEF2* | AB007860 | Hs.12802 | Development and differentiation enhancing factor | 1 |
| 1.42 | *Sec61g* | AA163916 | Mm.1164 | SEC61, γ-subunit (*S. cerevisiae*) | 1 |

Gene function was determined according to the Gene Ontology database. Gene symbol, gene name according to public databases; GenBank, identification number of the *c*DNA probe in the GenBank database; UniGene, cluster name in the UniGene database; product, gene common name; redundancy, number of spotted cDNA clones corresponding to the same gene. The genes without Genbank identification numbers and Unigene cluster names are private probes.

binding protein 2 (*Igfbp2*), forward 5′-CCTCAAGTCAGGCATGAAGGA-3′ and reverse 5′-GCAGGGAGTAGAGATGTTCCA-3′; β-actin (*Actb*), forward 5′-GAAATCGTGCGTGACATCAAAG-3′ and reverse 5′-TGTAGTTTCATGGATGCCACAG-3′; glycoprotein 38 (*GP38*), forward 5′-AGAGAACACGAGAGTACAACCA-3′ and reverse 5′-TGCGTTTCATCCCCTGCATT-3′; secretory leukocyte protease inhibitor (*Slpi*), forward 5′-CTGTTCCCATTCGCAAACCAG-3′ and reverse 5′-CCACATATACCCTCACAGCACTT-3′; activated leukocyte cell adhesion molecule (*Alcam*), forward 5′-ACGAAGAAAAGTGTGCAGTATGA-3′ and reverse 5′-ACTAGGGTAGGTGCTTCAAACA-3′; p21, forward 5′-GAAAACGGAGG-CAGACCAGC-3′ and reverse 5′-CACAGCAGAAGAGGGCGGG-3′; CD34, forward 5′-CAGCAGTAAGACCACACCAGC-3′ and reverse 5′-GGGGAAGTCTGTGGTTGTGAA-3′; inhibitor of DNA binding 2 (*Idb2*), forward 5′-AGAACCAGGCGTCCAGGAC-3′ and reverse 5-CTGCAAGGACAGGATGCTGA-3′; *Sca1*, forward 5′-ACCTATGCTGGTGGTCTGCC-3′ and reverse 5′-GACCAGAGCCTCTGGGTTGA-3′; transformed mouse 3T3 cell double minute 2 (*MDM2*), forward 5′-GTCTACCGAGGGTGCTGCAA-3′ and reverse 5′-TCCCCAGGTAGCTCATCTGTG-3′; ATP-binding cassette, subfamily B, member 4 (*Abcb4*), forward 5′-CTCAACACACGTCTAACAGATGA-3′ and reverse 5′-GATGAACCCCACTATGAATCCTG-3′; and ATP-binding cassette, subfamily A, member 8 (*ABCA8*), forward 5′-ACCCCAACAACTCAGAGGATAA-3′ and reverse 5′-CCACTACATCACTGAAACGCAT-3′.

## RESULTS

### *Isolation of C2C12 and C2CF6 SP and MP Cell Populations by Hoechst 33342 DNA Staining*

Hoechst 33342 staining was used to isolate SP and MP cell populations from the C2C12 murine muscle cell line expressing FGF6 or not as previously described (24) (Fig. 1). We were able to discriminate SP (S2) and MP (M2) fractions from C2C12, giving us around 0.5% of SP cells (0.01% with verapamil) (Fig. 1*A*). With the use of the C2CF6 cell line, we observed the same discrimination of SP (S6) and MP (M6) cell fractions with a significant increase of the SP cell fraction in the presence of FGF6 to up to 20% in average ($n = 6$) compared with the untransduced cells (Fig. 1*B*).

### *Expression Profiling of SP and MP Cells Isolated From C2C12 and C2CF6 Cell Lines*

DNA microarray technology was used to obtain an integrated view of the differential gene expression between SP and MP cells isolated from C2C12 and C2CF6 cell lines. The ANOVA method was first applied to identify and to quantitate systematic experimental biases as well as biological variabilities inherent to this kind of experiment. It was used as a basis for later normalization. Because all the experimental data are included in a single analysis, it benefits from a larger sample size than array-specific methods and leads to more robust statistical results and normalization processes.

The results showed important array, dye, biological condition, array × dye, and dye × gene effects for all biological samples that were compared. Because it is performed independently on each array, the lowess normalization method theoretically reduces the array × dye × gene effect, which does not appear explicitly in the ANOVA model used. In practice, it reduces both the dye × gene and array × dye effects (data not shown). It is used to diminish the well-known red-green imbalance in low intensities.

The second normalization process, based on the subtraction of significant main effects, can be considered as robust, because the mean values used for the correction are estimated over a large set of intensity values.

### *Accuracy and Robustness of the Experimental Data*

Figure 2*A* shows the accuracy of hybridization performed with the same cDNA target labeled with either Cy3 or Cy5.

Table 3. *Downregulated genes implicated in the FGF6 effect identified using ANOVA and differential analysis*

| Differential of Expression | Gene Symbol | GenBank Accession No. | Unigene | Product | Redundancy |
|---|---|---|---|---|---|
| | | | | *RNA synthesis* | |
| −8.74 | *H19* | X58196 | | H19 fetal liver mRNA | 1 |
| −3.47 | *Crap* | AF041847 | Mm.10279 | Cardiac-responsive adriamycin protein | 2 |
| −2.66 | *Ania4* | AF030089 | Rn.40517 | | 1 |
| −2.17 | *Ldb1* | U69270 | Mm.4524 | LIM domain binding 1 | 1 |
| −2.14 | *Jun* | J04115 | Mm.482 | Jun oncogene | 1 |
| −2.08 | *Sqstm1* | U57413 | Mm.200125 | Sequestosome 1 | 1 |
| −2.08 | *Vbp1* | U96760 | Mm.8294 | Von Hippel-Lindau binding protein 1 | 1 |
| −1.99 | *Rnps1* | X70067 | Mm.1951 | Ribonucleic acid binding protein S1 | 1 |
| −1.82 | *Hmgb3* | AF022465 | Mm.340 | High-mobility group box 3 | 1 |
| −1.81 | *Gata2* | AB000096 | Mm.1391 | GATA-binding protein 2 | 1 |
| −1.79 | *Paf53-pending* | D14336 | Mm.130322 | RNA polymerase l-associated factor | 1 |
| −1.61 | *Eif3* | X84651 | Mm.2238 | Eukaryotic translation initiation factor 3 | 2 |
| −1.53 | *Irf1* | M21065 | Mm.1246 | Interferon regulatory factor 1 | 1 |
| −1.52 | *Hdac2* | U31758 | Mm.19806 | Histone deacetylase 2 | 1 |
| −1.43 | *Rxrg* | X66225 | Mm.3475 | Retinold X receptor-γ | 1 |
| | | | | *Protein synthesis* | |
| −1.78 | *Rplp2* | X15098 | | Ribosomal protein, large $P_2$ | 1 |
| | | | | *Metabolism* | |
| −6.07 | *Ass1* | M31690 | Mm.3217 | Argininosuccinate synthetase 1 | 1 |
| −5.31 | *Alb1* | AJ011413 | Mm.16773 | Albumin 1 | 2 |
| −3.77 | *Vdac1* | U30840 | Mm.3555 | Voltage-dependent anion channel 1 | 2 |
| −3.21 | *Ctsd* | X52886 | Mm.2147 | Cathepsin D | 1 |
| −2.82 | *Acadm* | U07159 | Mm.10530 | Acetyl-CoA dehydrogenase, medium chain | 1 |
| −2.74 | *Sic39a1* | AF231120 | Mm.28756 | Solute carrier family 39 (zinc transporter), member 1 | 1 |
| −2.11 | *Gatm* | U07971 | Rn.33427 | Glycine amidinotransferase (L-arginine) | 2 |
| −2.03 | *Alp5a1* | NM_007505 | Mm.4069 | ATP synthase 5, α-subunit, isoform 1 | 1 |
| −1.92 | *Aldo1* | X03797 | | Aldolase 1, A isoform | 1 |
| −1.86 | *Atp2a2* | AF039893 | Mm.42255 | ATPase, $Ca^{2+}$-transporting, cardiac muscle, slow twitch 2 | 2 |
| −1.66 | *Apoa2* | X62772 | Mm.43677 | Apolipoprotein A-II | 1 |
| | | | | *Cell shape* | |
| −5.71 | *Acta2* | X13297 | Mm.16537 | Actin, $\alpha_2$, smooth muscle, aorta | 2 |
| −4.91 | *P4ha1* | U16162 | Mm.2212 | Proline 4-hydroxylase | 1 |
| −4.03 | *Tnni2* | J04992 | Mm.39469 | Troponin I, skeletal, fast 2 | 2 |
| −3.93 | *Acta1* | M12866 | Mm.214950 | Actin, $\alpha_2$, skeletal muscle | 3 |
| −3.65 | *Actb* | X03672 | Mm.297 | Actin, β, cytoplasmic | 2 |
| −3.21 | *Cnn2* | Z19543 | Mm.21776 | Calponin 2 | 1 |
| −2.66 | *COL5A2* | M11718 | Hs.82985 | | 1 |
| −2.60 | *Col1a1* | U08020 | Mm.22621 | Procollagen, type I, $\alpha_1$ | 1 |
| −2.56 | *Ptpns1* | D85785 | Mm.1682 | Protein lyrosine phosphatase, nonreceptor type substrate 1 | 1 |
| −2.49 | *Mylpf* | U77943 | Mm.14526 | Myosin light chain, phosphorylatable, fast skeletal muscle | 3 |
| −2.48 | *Col1a2* | X58251 | Mm.4482 | Procollagen, type I, $\alpha_2$ | 1 |
| −2.37 | *Tpm1* | M22479 | Mm.121878 | Tropomyosin 1, α | 6 |
| −2.28 | *Cappa2* | U16741 | Mm.3529 | Capping protein muscle Z-line, $\alpha_2$ | 1 |
| −2.02 | *Anxa6* | X13460 | Mm.22619 | Annexin $A_6$ | 1 |
| −1.84 | *Tncs* | AA572606 | Mm.1716 | Troponin C, fast skeletal | 1 |
| −1.80 | *Bgn* | NM_007542 | Mm.2608 | Biglycan | 1 |
| −1.71 | *Tnni1* | AJ242874 | Mm.36900 | Troponin I, skeletal, slow 1 | 1 |
| −1.71 | *Anxa3* | AA154734 | Mm.7214 | Annexin $A_3$ | 1 |
| −1.67 | *Actg2* | M26689 | Mm.16562 | Actin, $\gamma_2$ smooth muscle, enteric | 1 |
| −1.66 | *Tpm2* | X12650 | Mm.646 | Tropomyosin 2, β | 1 |
| −1.61 | *Prtn3* | U43525 | Mm.2364 | Proteinase 3 | 1 |
| −1.60 | *Adam12* | AI893930 | Mm.41158 | A disintegrin and metalloproteinase domain 12 (meltrin-α) | 1 |
| −1.52 | *Tpm3* | X53753 | Mm.17306 | Tropomyosin 3, γ | 1 |
| −1.42 | *Ptpn2* | M81477 | Mm.985 | Protein tyrosine phosphatase, non receptor type 2 | 1 |
| −1.41 | *TTN* | NM_003319 | Mm.46242 | Titin | 1 |
| | | | | *Cell signaling* | |
| −4.57 | *mcp-3* | | | Monocyte chemotactic protein 3 | 1 |
| −4.02 | *Akap12* | AB020886 | Mm.27481 | A kinase (PRKA) anchor protein (gravin) 12 | 1 |
| −3.69 | *Chma1* | AI385656 | Mm.4583 | Cholinergic receptor, nicotinic, α-polypeptide 1 (muscle) | 1 |
| −3.55 | *PPP3CB* | M29550 | Hs.151531 | Calcineurin A-β | 1 |
| −2.97 | *Ifngr* | M28233 | Mm.549 | Interferon γ receptor | 1 |

*Continued*

Table 3. *continued*

| Differential of Expression | Gene Symbol | GenBank Accession No. | Unigene | Product | Redundancy |
|---|---|---|---|---|---|
| −2.92 | *Dnajc3* | U28423 | Mm.12616 | DnaJ (Hsp40) homolog, subfamily C, member 3 | 1 |
| −2.80 | *Tnc* | AA003942 | Mm.980 | Tenascin C | 1 |
| −2.65 | *Pacsin2* | AF128535 | Mm.23978 | Protein kinase C and casein kinase substrate in neurons 2 | 1 |
| −2.62 | *Scarb2* | AB008553 | Mm.39288 | Scavenger receptor class B, member 2 | 1 |
| −2.55 | *Rsu1* | X63039 | Mm.905 | Ras suppressor protein 1 | 1 |
| −2.44 | *Sh3gl1* | U58885 | Mm.1773 | SH3-domain GRB2-like 1 | 1 |
| −2.43 | *Csk* | U05247 | Mm.21974 | c-Src tyrosine kinase | 1 |
| −2.34 | *Cd164* | AB028895 | Mm.28083 | CD164 antigen | 1 |
| −2.14 | *Osf2-pending* | D13664 | Mm.10681 | Osteoblast-specific factor 2 (fasciclin I-like) | 4 |
| −2.00 | *Calr* | M92988 | Mm.1971 | Calreticulin | 1 |
| −1.96 | *Narg1* | AF237622 | Mm.28256 | NMDA receptor-regulated gene 1 | 1 |
| −1.91 | *marcks* | NM_008538 | Mm.30059 | Myristoylated alanine-rich protein kinase C substrate | 2 |
| −1.89 | *Smo* | AF089721 | Mm.29279 | Smoothened homolog (*Drosophila*) | 1 |
| −1.79 | *Mlp* | AA154597 | Mm.2769 | MARCKS-like protein | 1 |
| −1.65 | *Tank* | U51907 | Mm.1803 | TRAF family member-associated NF-κB activator | 1 |
| −1.63 | *Cdh1* | X06115 | Mm.35605 | Cadherin 1 | 1 |
| −1.57 | *MAPKK4* | | | MAPK kinase 4 | 1 |
| −1.57 | *Il9r* | MB4746 | Mm.384 | Interleukin 9 receptor | 1 |
| −1.49 | *Rab1* | Y00094 | Mm.14530 | RAB1, member of the RAS oncogene family | 1 |
| −1.42 | *PPP2R5A* | NM_006243 | Hs.155079 | | 1 |
| −1.40 | *Kras* | | | Kras oncogene | 1 |
| | | | | *Cell division* | |
| −6.44 | *Igfbp2* | AI892100 | Mm.141936 | IGF binding protein 2 | 1 |
| −4.37 | *Igfbp7* | AB012886 | Mm.534 | IGF binding protein 7 | 1 |
| −3.44 | *Ccni* | AF005886 | Mm.22711 | Cyclin I | 2 |
| −2.50 | *Nmyc1* | M36277 | Mm.16469 | Neuroblastoma myc-related oncogene 1 | 1 |
| −2.42 | *Mcmd7* | D26091 | Mm.18923 | Minichromosome maintenance deficient 7 (*S. cerevisiae*) | 1 |
| −2.27 | *Tnfrsf11a* | AF019046 | Mm.6251 | Tumor necrosis factor receptor superfamily, member 11a | 1 |
| −2.09 | *Il11* | U03421 | Mm.35814 | Interleukin 11 | 1 |
| −1.81 | *Cdc10* | AF142759 | Rn.48701 | | 1 |
| −1.81 | *Cdkn2b* | AF059567 | Mm.8924 | Cyclin-dependent kinase inhibitor 2B (p15, inhibits CDK4) | 1 |
| −1.71 | *Ptma* | X56135 | Mm.19187 | Prothymosin-α | 1 |
| −1.61 | *Rtn4* | NM_031831 | Mm.220966 | Reticulon 4 | 1 |
| −1.60 | *Idb2* | M69293 | Mm.1466 | Inhibitor of DNA binding 2 | 1 |
| −1.58 | *p53* | | | p53 | 1 |
| −1.56 | *Cdkn1a* | AA072841 | Mm.34446 | Cyclin-dependent kinase inhibitor 1A (p21) | 1 |
| | | | | *Cell defense* | |
| −2.69 | *Hspa1l* | D85732 | Mm.14287 | Heat shock protein 1-like | 1 |
| −1.98 | *Serpinh1* | J05609 | Mm.22708 | Serine (or cysteine) proteinase inhibitor, clade H, member 1 | 1 |
| −1.89 | *Gstm2* | J04696 | Mm.14601 | Glutathione *S*-transferase, $\mu_2$ | 1 |
| −1.63 | *Cmkor1* | AF000236 | Mm.6522 | Chemokine orphan receptor 1 | 1 |
| −1.54 | *Ccr1* | U29678 | Mm.57051 | Chemokine (C-C motif) receptor 1 | 1 |
| −1.50 | *ARS2* | AF082871 | Mm.27932 | Arsenate resistance protein 2 | 1 |
| −1.42 | *Ada* | M10319 | Mm.388 | Adenosine deaminase | 1 |
| | | | | *Miscellaneous* | |
| −3.87 | *F3* | M26071 | Mm.3742 | Coagulation factor III | 1 |
| −3.16 | *Cct6a* | Z31557 | Mm.153159 | Chaperonin subunit 6a (ζ) | 3 |
| −2.70 | *Dmbt1* | U37438 | Mm.4138 | Deleted in malignant brain tumors 1 | 1 |
| −1.96 | *Ktn1* | L43326 | Mm.3110 | Kinectin 1 | 1 |
| −1.73 | *a* | L06451 | Mm.1890 | Nonagouti | 1 |
| −1.67 | *Pcbp2* | X75947 | Mm.111 | Poly(rC) binding protein 2 | 1 |
| −1.66 | *Sacm1l* | AB020658 | Mm.796 | SAC1 (supressor of actin mutations 1, homolog)-like (*S. cerevisiae*) | 1 |
| −1.63 | *Cct3* | Z31556 | Mm.3576 | Chaperonin subunit 3 (γ) | 1 |
| −1.62 | *Adprl2* | AJ007780 | Mm.5728 | ADP-ribosyltransferase [$NAD^+$: poly(ADP-ribose) polymerase]-like 2 | 1 |
| −1.61 | *Nedd4a* | U96635 | Mm.16553 | Neural precursor cell expressed, developmentally downregulated gene 4 | 1 |
| −1.60 | *Pxmp3* | AF031128 | Mm.16453 | Peroxisomal membrane protein 3 | 1 |
| −1.57 | *Ucp2* | U69135 | Mm.144413 | Uncoupling protein 2, mitochondrial | 1 |
| −1.54 | *Krt1-16* | AF053235 | Mm.19889 | Keratin complex 1, acidic, gene 16 | 1 |
| −1.45 | *Rnaseh1* | AF048993 | Mm.10152 | Ribonuclease $H_1$ | 1 |

This plot represents the differential scores obtained for all the probes involved in the experiment, sorted in the ascending order. The region of acceptance of H0 (no differential expression) is between the upper and lower 1, 5, 10, 15, or 20% type I error rate thresholds, according to the false positive rate that we are ready to accept. At the level of the 20% error rate, 99% of the differential scores fall within these thresholds, meaning that there are 2 of 7,200 (0.03%) false positives. The same

Table 4. *Upregulated genes implicated in the differentiation effect identified using global ANOVA and differential analysis*

| Differential of Expression | Gene Symbol | Genbank Accession No. | Unigene | Product | Redundancy |
|---|---|---|---|---|---|
| | | | | *RNA synthesis* | |
| 3.57 | *Nfe2l2* | U20532 | Mm.1025 | Nuclear factor, erythroid-derived 2, like 2 | 1 |
| 3.11 | *Aes* | AA153668 | Mm.2626 | Amino-terminal enhancer of split | 1 |
| 2.53 | *Sqstm1* | U57413 | Mm.200125 | Sequestosome 1 | 1 |
| 1.96 | *Nfatc2* | U02079 | Mm.116802 | Nuclear factor of activated T cells, cytoplasmic 2 | 1 |
| 1.66 | *Pitx2* | U80010 | Mm.1385 | Paired-like homeodomain transcription factor 2 | 1 |
| 1.47 | *Sfrs5* | AF020683 | Mm.43331 | Splicing factor, arginine-serine-rich 5 | 1 |
| 1.42 | *Tgif* | AA060371 | Mm.8155 | TG interacting factor | 1 |
| | | | | *Protein synthesis* | |
| 2.10 | *Eif3* | X84651 | Mm.2238 | Eukaryotic translation initiation factor 3 | 1 |
| 1.63 | *Ubl1* | AF033353 | Mm.7353 | Ubiquitin-like 1 | 1 |
| | | | | *Metabolism* | |
| 2.91 | *Slc20a1* | M73696 | Mm.16757 | Solute carrier family 20, member 1 | 1 |
| 2.79 | *Acadm* | U07159 | Mm.10530 | Acetyl-CoA dehydrogenase, medium chain | 1 |
| 2.56 | *Gpd2* | D50430 | Mm.3711 | Glycerol phosphate dehydrogenase 2, mitochondrial | 1 |
| 2.27 | *Idh1* | AI325900 | Mm.9925 | Isocitrate dehydrogenase 1 ($NADP^+$), soluble | 1 |
| 1.90 | *Acad1* | U21489 | Mm.2445 | Acetyl-CoA dehydrogenase, long-chain | 1 |
| 1.75 | *Atp5a1* | NM_007505 | Mm.4069 | ATP synthase, mitochondrial F1 complex, α-subunit, isoform 1 | 1 |
| 1.62 | *Adss1* | M74495 | Mm.3440 | Adenylosuccinate synthetase 1, muscle | 1 |
| 1.54 | *Ass1* | M31690 | Mm.3217 | Argininosuccinate synthetase 1 | 1 |
| 1.44 | *Aldo3* | W09791 | Mm.7729 | Aldolase 3, C isoform | 1 |
| | | | | *Cell shape* | |
| 1.96 | *Cnn2* | Z19543 | Mm.21776 | Calponin 2 | 1 |
| 1.76 | *P4ha1* | U16162 | Mm.2212 | Procollagen-proline, 2-oxoglutarate 4-dioxygenase, $\alpha_1$-polypeptide | 1 |
| 1.74 | *Gsn* | J04953 | Mm.227050 | Gelsolin | 1 |
| 1.56 | *MEF2C* | | | Myocyte enhancer factor 2C | 1 |
| | | | | *Cell signaling* | |
| 3.03 | *Ikbalpha* | | | I-κB-α | 1 |
| 2.76 | *Vdac1* | U30840 | Mm.3555 | Voltage-dependent anion channel 1 | 1 |
| 2.57 | *MCP-3* | | | Monocyte Chemotactic protein 3 | 1 |
| 2.40 | *Ifngr* | M28233 | Mm.549 | Interferon γ receptor | 1 |
| 2.31 | *Igf2r* | U04710 | Mm.2938 | IGF 2 receptor | 1 |
| 2.14 | *Arhgef7* | U96634 | Mm.3439 | Rho guanine nucleotide exchange factor (GEF7) | 1 |
| 1.89 | *Arhc* | X80638 | Mm.262 | Ras homolog gene family, member C | 1 |
| 1.76 | *Oprs1* | AF030198 | Mm.22745 | Opioid receptor, $\sigma_1$ | 1 |
| 1.67 | *Rras* | M21019 | Mm.257 | Harvey rat sarcoma oncogene, subgroup R | 1 |
| 1.55 | *Gpld1* | AF050666 | Mm.2779 | Glycosylphosphatidytinositolspecific phospholipase $D_1$ | 1 |
| 1.46 | *Ntrk3* | AF035400 | Mm.20467 | Neurotrophic tyrosine kinase, receptor, type 3 | 1 |
| 1.41 | *Psap* | S36200 | Mm.233010 | Prosaposin | 2 |
| | | | | *Cell division* | |
| 4.16 | *Gm* | M86736 | Mm.1568 | Granulin | 2 |
| 3.57 | *Ccni* | AF005886 | Mm.22711 | Cyclin 1 | 2 |
| 3.55 | *Ccnb2* | X66032 | Mm.22592 | Cyclin $B_2$ | 1 |
| 2.73 | *p53* | | | p53 | 1 |
| 2.10 | *Mcl1* | U35623 | Mm.1639 | Myeloid cell leukemia sequence 1 | 1 |
| 1.96 | *Ctsd* | X52886 | Mm.2147 | Cathepsin D | 1 |
| 1.54 | *Ccnd1* | AI894115 | Mm.22288 | Cyclin $D_1$ | 1 |
| 1.53 | *Cdkn2b* | AF059567 | Mm.8924 | Cyclin-dependent kinase inhibitor 2B (p15. inhibits CDK4) | 1 |
| 1.46 | *Idb2* | M69293 | Mm.1466 | Inhibitor of DNA binding 2 | 2 |
| 1.45 | *Hmgn2* | X12944 | Mm.911 | High-mobility group nucleosomal binding domain 2 | 1 |
| 1.43 | *p21* | | | p21 | 1 |
| | | | | *Cell defense* | |
| 5.09 | *Gstm2* | J04696 | Mm.14601 | Glutathione *S*-transferase, $\mu_2$ | 1 |
| 2.32 | *Gstm1* | J04632 | Mm.2011 | Glutathione *S*-transferase, $\mu_1$ | 1 |
| 2.17 | *Ccr6* | AB016031 | Mm.8007 | Chemokine (C–C motif) receptor 6 | 1 |
| 2.15 | *Hspa5* | D78645 | Mm.918 | Heat shock 70kD protein 5 (glucose-regulated protein) | 1 |
| 2.06 | *Ly6c* | AA024002 | Mm.1583 | Lymphocyte antigen 6 complex, locus C | 2 |
| 1.90 | *Irf1* | M21065 | Mm.1246 | Interferon regulatory factor 1 | 1 |
| 1.72 | *H2-K* | L36312 | Mm.16771 | Histocompatibility 2, K region | 2 |
| 1.68 | *Gsta4* | L06047 | Mm.2662 | Glutathione *S*-transferase, $\alpha_4$ | 1 |

*Continued*

Table 4. *continued*

| Differential of Expression | Gene Symbol | Genbank Accession No. | Unigene | Product | Redundancy |
|---|---|---|---|---|---|
| 1.53 | *Il9r* | M84746 | Mm.384 | Interleukin 9 receptor | 1 |
| 1.50 | *Ly6a* | Al325697 | Mm.8180 | Lymphocyte antigen 6 complex, locus A | 1 |
| | | | | *Miscellaneous* | |
| 3.65 | *Dusp1* | X61940 | Mm.2404 | Dual-specificity phosphatase 1 | 1 |
| 3.14 | *Ptgs1* | M34141 | Mm.2792 | Prostaglandin-endoperoxide synthase 1 | 1 |
| 2.86 | *Scarb2* | AB008553 | Mm.39288 | Scavenger receptor class B, member 2 | 1 |
| 2.64 | *F3* | M26071 | Mm.3742 | Coagulation factor III | 1 |
| 2.39 | *Zfp216* | AF062071 | Mm.2904 | Zinc finger protein 216 | 1 |
| 2.10 | *Pxmp3* | AF031128 | Mm.16453 | Peroxisomal membrane protein 3 | 1 |
| 2.00 | *Mcmd7* | D26091 | Mm.18923 | Minichromosome maintenance deficient 7 (*S. cerevisiae*) | 1 |
| 1.99 | *Grpel2* | AF041060 | Mm.12959 | GrpE-like 2, mitochondrial | 1 |
| 1.99 | *Ctsz* | AJ242663 | Mm.156919 | Cathepsin Z | 1 |
| 1.94 | *Cryz* | D78646 | Mm.3534 | Crystallin, ζ | 1 |
| 1.83 | *Cd34* | AI893233 | Mm.29798 | CD34 antigen | 1 |
| 1.71 | *Sh3gl1* | U58885 | Mm.1773 | SH3-domain GRB2-like 1 | 1 |
| 1.67 | *Tiegl* | AA144487 | Mm.4292 | TGFB-inducible early growth response 1 | 1 |
| 1.56 | *ler2* | AI325877 | Mm.399 | Immediate-early response 2 | 1 |
| 1.52 | *Ldtr* | AA119521 | Mm.3213 | Low-density lipoprotein receptor | 1 |
| 1.50 | *Sat* | L10244 | Mm.2734 | Spermidinespermine *N*1-acetyl transferase | 1 |
| 1.50 | *Lxn* | AA170148 | Mm.2632 | Latexin | 2 |
| 1.42 | *Ucp2* | AA169003 | Mm.144413 | Uncoupling protein 2, mitochondrial | 2 |

conclusion can be drawn from the experiment using hybridization of the same sample after RNA amplification (Fig. 2*B*) with 10 of 7,200 (0.07%) false positives at the level of the 20% error rate. The threshold value to determine genes differentially expressed is inversely proportional to the square root of the number of dye swaps involved in the experiment. Thus, as the number of replicates increases, the decision threshold decreases, resulting in a larger number of genes that are found to be significantly differentially expressed.

To evaluate the reproducibility of the experimental process, we used a set of triplicate experiments (*experiments A–C*) on six arrays hybridized in dye swap and on which the same two conditions were compared. According to the whole process of normalization and differential analysis described above, each dye swap was first analyzed separately. Three pools of two dye swaps were then formed, and, finally, the six arrays were pooled together. For five genes found to be differentially expressed in the seven analyses, a *P* value was calculated according to the statistical model used to describe the differential scores. Figure 3 shows the evolution of the *P* value for these genes as the number of arrays involved in the analysis increased. The first three points correspond to the *P* value obtained from single swap analyses (*A–C*); the fourth, fifth, and sixth values were obtained with duplicates (*A*+*B*, *A*+*C*, and *B*+*C*); and the last one corresponds to the analysis with a triplicate (*A*+*B*+*C*). For those genes that were found to be differentially expressed in all cases, the *P* value reduced drastically and stabilized when two swaps were pooled for the analysis. Pooling three replicates strengthens the conclusions and increased the number of genes that were found to be differentially expressed (data not shown).

### *Individual Expression Profiling*

Expression profiling was performed for each experiment to extract specific sets of genes with differential expression between cell populations. As a control of specificity, RNAs of C2C12 or C2CF6 cells treated or not with Hoechst 33342 without sorting were purified, and the cDNA targets derived from them were analyzed through a microarray experiment to investigate the effect of Hoechst dye on the cells. No statistically significant modulation was observed (data not shown). This result validates the specificity of the modulation described. To explore the transcriptome of the four cell populations (M2, M6, S2, and S6), ANOVA, a normalization, and a differential analysis were first successively performed for each of the six paired comparisons independently (M2/M6, M2/S2, M2/S6, S2/S6, M6/S2, and M6/S6).

Thus genes with up- and downregulated expression were identified for all hybridization conditions, and the distribution of the number of genes does not indicate a significant global imbalance of transcriptionally modulated genes between each comparison (data not shown).

The functional analysis of these genes, presented in Table 1, indicates that the majority of them are involved in biological processes such as RNA synthesis (9%), metabolism (27%), cell shape (16%), cell signaling (17%), cell division (14%), and cell defense (4%). Interestingly, the genes involved in the shape of the cell (matrix, cytoskeletal, and muscular markers) were preferentially downregulated in the M6, S2, and S6 cell fractions compared with the M2 cell fraction. This suggests a more undifferentiated phenotype of these cells. In addition, no significant variation of the expression of cell shape-related genes was observed between the S2, S6, and M6 fractions, suggesting a similar undifferentiated phenotype of these cells in relation to these molecular markers.

### *Global Analysis*

Such a two-by-two analysis identifies modulated genes in each experiment but does not allow simple discrimination of genes with expression either modulated specifically by FGF6 or characteristic of the difference between MP and SP cells. Analyses were performed on the whole data set composed of the six individual comparisons (M2/M6, M2/S2, M2/S6, S2/S6, M6/S2, and M6/S6) to extract the two sets of genes that

Table 5. *Downregulated genes implicated in the differentiation effect identified using global ANOVA and differential analysis*

| Differential of Expression | Gene Symbol | GenBank Accession No. | Unigene | Product | Redundancy |
|---|---|---|---|---|---|
| | | | | *RNA synthesis* | |
| −3.15 | *Ldb1* | U69270 | Mm.4524 | LIM domain binding 1 | 1 |
| −1.97 | *Rpo1-3* | D86609 | Mm.34570 | RNA polymerase 1–3 | 1 |
| −1.48 | *Polr2g* | AA140026 | Mm.22117 | Polymerase (RNA) II (DNA directed) polypeptide G | 1 |
| | | | | *Protein synthesis* | |
| −2.94 | *Psmb8* | U22031 | Mm.13913 | Proteosome (prosome, macropain) subunit, β-type 8 | 1 |
| −2.06 | *Uble1a* | AB024303 | Mm.29698 | Ubiquitin-like 1 (sentrin)-activating enzyme E1A | 1 |
| −1.97 | *Psme3* | D87911 | Mm.2141 | Proteaseome (prosome, macropain) 28 subunit, 3 | 1 |
| −1.90 | *Psmb7* | D83585 | Mm.2246 | Proteasome (prosome, macropain) subunit, β-type 7 | 1 |
| −1.48 | *Eif4g2* | U76112 | Mm.525 | Eukaryotic translation initiation factor 4, $\gamma_2$ | 1 |
| | | | | *Metabolism* | |
| −2.88 | *Stpi* | AI324399 | Mm.1395 | Secretory leukocyte protease inhibitor | 2 |
| −2.63 | *Abcb4* | J03398 | Mm.14172 | ATP-binding cassette, sub family B (MDRTAP), member 4 | 1 |
| −2.49 | *Arf6* | D87903 | Mm.196526 | ADP ribosylation factor 6 | 1 |
| −2.17 | *Ppil1* | AA139313 | Mm.196081 | Peptidylprolyl isomerase (cyclophilin)-like 1 | 1 |
| −1.94 | *Npm1* | AA170528 | Mm.6343 | Nucleophosmin 1 | 1 |
| −1.84 | *Furin* | AA152814 | Mm.5241 | Furin (paired basic amino acid-cleaving enzyme) | 1 |
| −1.72 | *Amd2* | NM_007444 | Mm.195848 | *S*-adenosylmethionine decarboxylase 2 | 1 |
| −1.60 | *Fxyd5* | U72680 | Mm.1870 | FXYD domain-containing ion transport regulator 5 | 1 |
| −1.56 | *Dhfr* | AA008267 | Mm.23695 | Dihydrofolate reductase | 1 |
| −1.55 | *Impdh2* | M33934 | Mm.6065 | Inosine 5′-phosphate dehydrogenase 2 | 1 |
| −1.54 | *Cyp2b19* | AF047529 | Mm.14098 | Cytochrome P450, family 2, subfamily b, polypeptide 19 | 1 |
| −1.53 | *Slc39a1* | AF231120 | Mm.28756 | Solute carrier family 39 (zinc transporter), member 1 | 1 |
| −1.49 | *Alp5c1* | L19927 | Mm.12677 | ATP synthase, mitochondrial F1 complex, γ-polypeptide 1 | 2 |
| −1.49 | *Cyp3a16* | D26137 | Mm.30303 | Cytochrome P450, family 3, subfamily a, polypeptide 16 | 1 |
| −1.42 | *A.enol* | | | α-Enolase | 1 |
| −1.41 | *Pitpn* | AI327361 | Mm.3128 | Phosphatidylinositol transfer protein | 1 |
| | | | | *Cell shape* | |
| −4.47 | *Mylpf* | U77943 | Mm.14526 | Myosin light chain, phosphorylatable, fast skeletal muscle | 3 |
| −3.43 | *Tnni2* | J04992 | Mm.39469 | Troponin I, skeletal, fast 2 | 3 |
| −3.03 | *Tncs* | AA572606 | Mm.1716 | Troponin C, fast skeletal | 1 |
| −2.56 | *Actb* | X03672 | Mm.297 | Actin, β, cytoplasmic | 1 |
| −2.43 | *Tpm1* | M22479 | Mm.121878 | Tropomyosin 1, α | 1 |
| −2.31 | *Acta2* | X13297 | Mm.16537 | Actin, $\alpha_2$, smooth muscle, aorta | 1 |
| −2.26 | *Adam12* | AI893930 | Mm.41158 | A disintegrin and metalloproteinase domain 12 (meltrin-α) | 1 |
| −1.92 | *Tnnl3* | U77779 | Mm.14546 | Troponin T3, skeletal, fast | 1 |
| −1.86 | *Anxa3* | AJ001633 | Mm.7214 | Annexin $A_3$ | 1 |
| −1.83 | *Mmp2* | M84324 | Mm.29564 | Matrix metalloproteinase 2 | 1 |
| −1.77 | *Col3A1* | | | Procollagen, type III, $\alpha_1$ | 1 |
| −1.74 | *Cotl1* | AI325867 | Mm.141741 | Coactosin-like 1 (*Dictyostelium*) | 1 |
| −1.70 | *Acta1* | M12866 | Mm.214950 | Actin, $\alpha_1$, skeletal muscle | 1 |
| −1.65 | *Tpm2* | M87635 | Mm.646 | Tropomyosin 2, β | 3 |
| −1.59 | *Smarcc1* | U85614 | Mm.1050 | SWI/SNF complex 155-kDa subunit | 1 |
| −1.57 | *Actn4* | AI327147 | Mm.143830 | Actinin $\alpha_4$ | 1 |
| −1.41 | *Adam10* | AF011379 | Mm.3911 | A disintegrin and metalloprotease domain 10 | 1 |
| | | | | *Cell signaling* | |
| −5.03 | *Rtkn* | U54638 | Mm.4139 | Rhotekin | 1 |
| −3.95 | *Cdh3* | X06340 | Mm.4658 | Cadherin 3 | 1 |
| −2.57 | *Rab7* | NM_009005 | Mm.4268 | RAB7, member of the RAS oncogene family | 1 |
| −2.41 | *Prkch* | D90242 | Mm.8040 | Protein kinase C, η | 1 |
| −2.21 | *Chma1* | AI385656 | Mm.4583 | Cholinergic receptor, nicotinic, α-polypeptide 1 | 1 |
| −1.96 | *Thbs2* | L07803 | Mm.26688 | Thrombospondin 2 | 1 |
| −1.92 | *Ltk* | X52621 | Mm.1740 | Leukocyte tyrosine kinase | 1 |
| −1.83 | *Epha7* | X81466 | Mm.4806 | Eph receptor A7 | 1 |
| −1.65 | *Itpr1* | AA155482 | Mm.2726 | Inositol 1,4,5-trisphosphate receptor 1 | 1 |
| −1.57 | *Cd68* | X68273 | Mm.15819 | CD68 antigen | 1 |
| −1.57 | *RAB14* | AF052113 | Mm.198264 | RAB14 member of the RAS oncogene family | 1 |
| −1.54 | *Fgfr4* | AI385693 | Mm.4912 | FGF receptor 4 | 1 |
| −1.54 | *Gfra2* | AF002701 | Mm.41886 | Glial cell line derived neurotrophic factor family receptor $\alpha_2$ | 1 |
| −1.52 | *PPP3CB* | M29550 | Mm.24381 | Protein phosphatase 3, catalytic subunit, β-isoform | 1 |
| −1.47 | *Gna13* | AA073262 | Mm.222695 | Guanine nucleotide binding protein, $\alpha_{13}$ | 1 |

*Continued*

Table 5. *continued*

| Differential of Expression | Gene Symbol | GenBank Accession No. | Unigene | Product | Redundancy |
|---|---|---|---|---|---|
| | | | | *Cell division* | |
| −3.48 | *mertk* | U21301 | Mm.4582 | C-mer proto-oncogene tyrosin kinase | 1 |
| −3.13 | *Axl* | X63535 | Mm.4128 | AXL receptor tyrosine kinase | 1 |
| −2.91 | *Scgf* | AB009245 | Mm.20428 | Stem cell growth factor | 1 |
| −2.40 | *Cyclin D3* | | | Cyclin $D_3$ | 1 |
| −2.22 | *Mdk* | W97681 | Mm.906 | Midkine | 1 |
| −1.99 | *Cdc2l1* | AI528628 | Mm.87864 | Cell division cycle 2 homolog (*S. pombe*)-like 1 | 1 |
| −1.89 | *Kif22* | AI325845 | Mm.29381 | Kinesin family member 22 | 1 |
| −1.81 | *cyclin D1* | | | Cyclin $D_1$ | 1 |
| −1.80 | *cycliin D2* | | | Cyclin $D_2$ | 1 |
| −1.77 | *Igfbp2* | AI892100 | Mm.141936 | IGF binding protein 2 | 1 |
| −1.71 | *Cdc2a* | AI893495 | Mm.4761 | Cell division cycle 2 homolog A (*S. pombe*) | 1 |
| −1.64 | *Rfc5* | AA142505 | Mm.27997 | Replication factor C (activator 1) 5 | 1 |
| −1.63 | *Pa2g4* | X84789 | Mm.4742 | Proliferation-associated 2G4 | 1 |
| −1.55 | *Stk18* | L29479 | Mm.3794 | Serine-threonine kinase 18 | 1 |
| −1.48 | *Fsp27* | AA062151 | Mm.10026 | Fat-specific gene 27 | 1 |
| −1.47 | *Ccnb1-rs1* | AA154813 | Mm.22569 | Cyclin $B_1$, related sequence 1 | 1 |
| −1.43 | *Mpdz* | AF000168 | Mm.3140 | Multiple PDZ domain protein | 1 |
| | | | | *Cell defense* | |
| −3.58 | *Il2ra* | M30856 | Mm.915 | Interleukin 2 receptor, α-chain | 1 |
| −2.80 | *Hspe1* | AA041628 | Mm.197601 | Heat shock protein 1 (chaperonin 10) | 3 |
| −2.19 | *H2-Oa* | M95514 | Mm.116 | Histocompatibility 2, O region, α-locus | 2 |
| −1.61 | *Serpinb2* | AI323222 | Mm.5019 | Serine (or cysteine) proteinase inhibitor, clade B, member 2 | 1 |
| −1.43 | *Mgmt* | AA271071 | Mm.1216 | *O*-6-methylguanine-DNA methyltransferase | 1 |
| | | | | *Miscellaneous* | |
| −2.28 | Tctex1 | AA155514 | Mm.1948 | T complex testis expressed 1 | 1 |
| −2.23 | Myd116 | AA155095 | Mm.4048 | Myeloid differentiation primary response gene 116 | 1 |
| −1.92 | Nedd1 | D10712 | Mm.2998 | Neural precursor cell expressed, developmentally downregulated gene 1 | 1 |
| −1.75 | Top2a | U01915 | Mm.4237 | Topoisomerase (DNA) II-α | 1 |
| −1.74 | Nucb | M96823 | Mm.2283 | Nucleobindin | 1 |
| −1.74 | Dnajb10 | AI322546 | Mm.103605 | DnaJ (Hsp40) homolog, subfamily B, member 10 | 1 |
| −1.68 | Trim27 | AA162497 | Mm.55 | Tripartite motif protein 27 | 1 |
| −1.62 | Atp1b3 | AA139067 | Mm.424 | ATPase, $Na^+$, $K^+$ transporting, β-polypeptide | 1 |
| −1.51 | Nup210 | W99187 | Mm.28162 | Nucleoporin 210 | 1 |
| −1.51 | Fbl | AI325773 | Mm.4595 | Fibrillarin | 1 |
| −1.47 | Ssfa1 | AA146251 | Mm.29504 | Sperm-specific antigen 1 | 1 |
| −1.43 | Gp38 | M73748 | Mm.2976 | Glycoprotein 38 | 1 |
| −1.43 | Cct6a | AI324947 | Mm.153159 | Chaperonin subunit 6a (ζ) | 1 |

best characterized either the FGF6 effect or the difference between SP and MP cells. Thus a PCA was performed to provide a projection of the data set in a new space of reduced size and to visualize its structure. A table was filled in with the differential scores computed previously for each gene in each of the six experiments, with the genes in lines and the experiments in columns. Missing values, corresponding to flagged genes, were replaced by random values taken from a normal distribution with a mean of 0 and a standard deviation of 0.02. These random values correspond to a situation of constant expression in the corresponding experiment. The resulting table was used as input to the PCA (not shown).

In the first case, the complete set of validated genes was used (5,654 genes). In the second case, the PCA table was restricted to genes that had been found differentially expressed in at least one of the six experiments (297 genes). In both cases, the resulting cluster was centered on a core of genes with little (or no) differential expression, whereas the most modulated genes behaved as "outliers" and were located outside, as shown in Fig. 4. Superimposed on this data cluster were the six directions associated with the six experiments (or variables). A simultaneous analysis of the data set and variables pointed out the genes that best characterized either each experiment or a set of experiments. Here, outliers define three distinct directions. The colinear axis (Fig. 4) to the direction M2/M6 and S2/S6 distinguishes genes that characterized the FGF6 effect independently of their phenotypic link (SP or MP). At one extremity are the most upregulated genes, and at the other one are the most downregulated ones. The second axis is derived from the S2/M2 and S6/M2 directions defined by genes with modulated expression between the M2 and S2/S6 cell fractions. It corresponds to a "differentiation" effect from differentiated M2 cells to less-differentiated S2/S6 cells.

As indicated on Fig. 4, a third axis could be built from the S2/M2 and S6/M6 directions defined by genes with modulated expression between the SP and MP cell fractions independently of the presence of FGF6. This axis should correspond to a "Hoechst" or "population" effect, but the similarity of the genes implicated in this effect compared with those implicated in the differentiation effect brought us to consider only two main contributions: the FGF6 and differentiation effects.

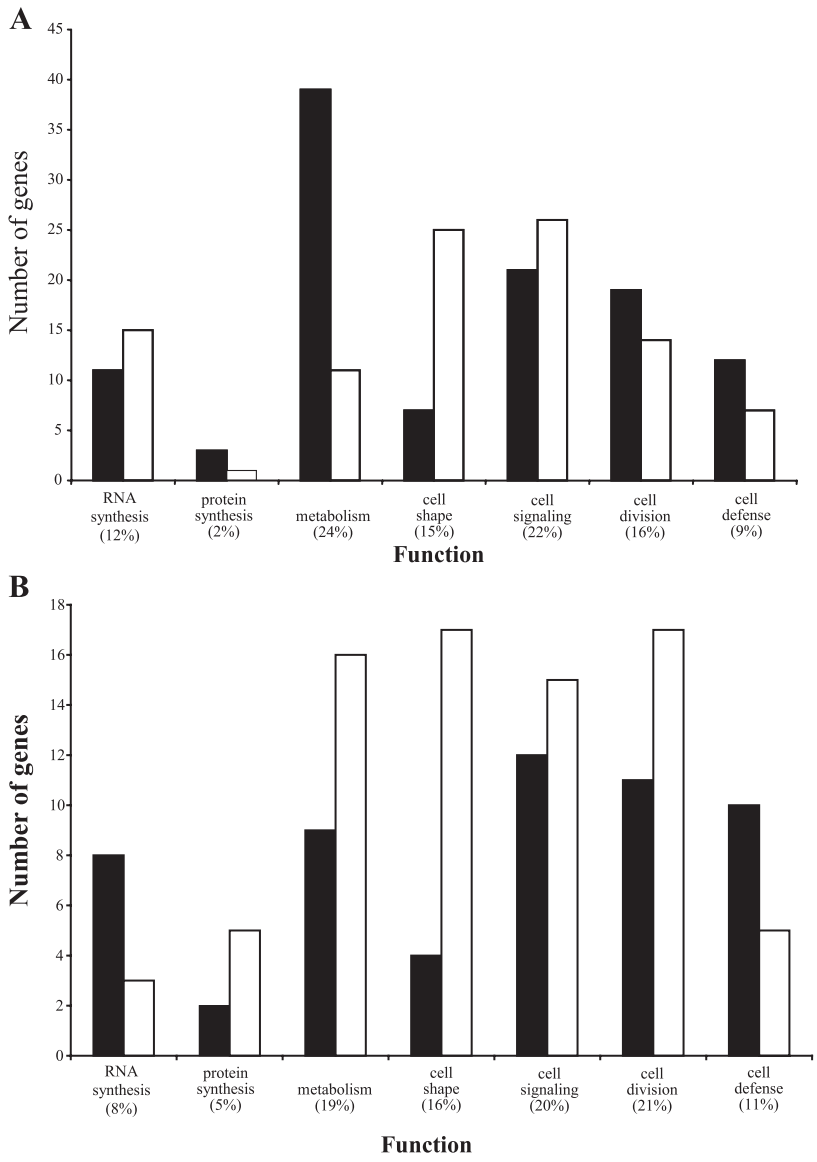


Fig. 5. Distribution of upregulated (solid bars) and downregulated genes (open bars) as a function of their biological function identified in the Gene Ontology database. *A*: genes implicated in the FGF6 effect. *B*: genes implicated in the differentiation effect.

The S2/S6 direction almost follows the FGF6 axis as defined above (Fig. 4). Thus this indicates that there are no significant differences between these two cell fraction transcriptomes in relation to the 7,690 molecular markers present in our study, showing that these cells have a similar SP phenotype.

To confirm the descriptive results obtained by PCA, we performed ANOVA and a differential analysis on the two subsets of hybridizations. The genes up- or downregulated in FGF6-treated cells compared with untreated cells were labeled as genes preferentially modulated by FGF6 or implicated in the FGF6 effect; the genes upregulated or downregulated in SP compared with MP cells were labeled as genes preferentially implicated in the differentiation effect. Thus 511 genes were highlighted with a $P$ value $<0.20$ according to a FGF6 effect and 322 genes according to a differentiation effect. The results presented in Tables 2 and 3 show the 250 genes, with annotated function, with expression regulated in response to the presence of FGF6. Tables 4 and 5 present the 164 annotated genes preferentially implicated in the differentiation effect.

*FGF6 effect.* A total of 137 genes with known functions is specifically upregulated (Table 2) and a total of 113 genes is downregulated by FGF6 (Table 3). Among them, FGF6 (positive control) was normally upregulated in the M6 and S6 cell fractions compared with the M2 and S2 cell fractions (data not shown).

The distribution of these genes, accordingly to seven main cellular functions (RNA synthesis, protein synthesis, metabolism, cell shape, cell signaling, cell division, and cell defense) is presented in Fig. 5*A* and shows the modulation of four principal functions: metabolism (24%), cell shape (15%), cell signaling (22%), and cell division (16%).

*Differentiation effect.* A total of 73 genes with known functions is specifically upregulated (Table 4) and a total of 91 genes is downregulated (Table 5) in SP compared with MP cells. The distribution of these genes, accordingly to their cellular function, is presented in Fig. 5*B* and shows the modulation of four main cellular functions: metabolism (19%), cell shape (16%), cell signaling (20%), and cell division (21%).

Table 6. *Real-time RT-PCR analysis of genes implicated in the FGF6 and differention effects identified using global ANOVA and differential analysis*

| Gene Symbol | Ratio M6 vs. M2 | Ratio S2 vs. M2 |
|---|---|---|
| | *FGF6 effect* | |
| Down regulated genes | | |
| *Acta1* | 0.01 | |
| *Idb2* | 0.02 | |
| *Igfbp2* | 0.20 | |
| *Actb* | 0.30 | |
| Up regulated genes | | |
| *ABCA8* | 23.95 | |
| *Slpi* | 9.70 | |
| *Abcg4* | 9.10 | |
| *GP38* | 3.20 | |
| *Sca1* | 1.97 | |
| *Alcam* | 1.80 | |
| *MDM2* | 1.80 | |
| *CD34* | 1.25 | |
| *FGF6* | 15.20 | |
| | *Differentiation effect* | |
| Down regulated genes | | |
| *GP38* | | 0.60 |
| *Slpi* | | 0.60 |
| Upregulated genes | | |
| *p21* | | 2.03 |
| *CD34* | | 1.80 |
| *Sca1* | | 1.30 |
| *Idb2* | | 1.30 |

*Microarray experimental data validation by real-time RT-PCR.* We performed real-time RT-PCR for 14 genes to confirm both the FGF6 and differentiation effects (Table 6). To validate the FGF6 effect, we confirmed the downregulation of *Acta1*, *Idb2*, *Igfbp2*, and *Actb* in M6 versus M2 cell fractions and the upregulation of *ABCA8*, *Slpi*, *Abcg4*, *GP38*, *Sca1*, *Alcam*, *MDM2*, *CD34*, and the control gene *FGF6* in M6 versus M2 cell fractions. Moreover, for *Myd116*, we observed weak upregulation in M6 versus M2 cell fractions and strong upregulation in S6 versus M2 cell fractions (not shown) and observed an upregulation of *Sca1* expression in M6 versus M2 cell fractions not detected by the microarray.

To validate the differentiation effect, we confirm the downregulation of *GP38* and *Slpi* in S2 versus M2 cell fractions and the upregulation of *p21*, *CD34*, *Sca1*, and *Idb2* in S2 versus M2 cell fractions.

Real-time RT-PCR was not suitable to confirm the expression modulations observed in S6 versus M2 cell fractions, which combines both the FGF6 and differentiation effects.

## DISCUSSION

In this study, we compared gene expression profiles from cells with SP and MP phenotypes derived from the C2C12 muscle cell line in the presence or absence of FGF6.

Many factors have been shown to act upon the process of satellite cell activation and recruitment, such as IGF-1, leukemia inhibitory factor, IL-6, and FGF6. In particular, it has been shown that knockout of FGF6 in normal mice leads to severely defective muscle regeneration and, in the mdx mouse, to a considerable aggravation of the dystrophic phenotype with diminished expression of MyoD at sites of necrosis-regeneration and a concomitant accumulation of interstitial collagen (16). FGF6 is specifically produced by muscle fibers and both promotes cell proliferation and counteracts cell apoptosis.

On the other hand, FGF6 also gives rise to multiple effects depending on its concentration. At 5 ng/ml, it promotes differentiation of myogenic precursors (38). At 25 ng/ml, FGF6 acts as a muscle proliferation agent and delays differentiation of muscle precursors (38). At about 100 ng/ml, we have shown that this growth factor reduces cell growth while increasing the proportion of cells with the SP phenotype (23). These unique features designate FGF6 as a key factor in muscle regeneration. Therefore, we decided to perform global transcriptional profiling to examine FGF6 for its capacity to either increase or mobilize the pool of immature muscle cells. In the presence of high concentrations of FGF6 (up to 75–100 ng/ml), the proportion of SP cells (S6) was tremendously increased. As we (23) have previously described, C2CF6 differs from the original C2C12 cell line: C2CF6 cells are more likely to divide and have increased resistance to apoptosis. Moreover, they never reach a confluent state and do not fuse to form myotubes. They also display severe downregulation of expression of some important myogenic regulatory factors such as MyoD and myogenin.

With the use of microarray technology coupled with robust statistical analysis of the data, we identified genes involved in the FGF6 cell response. Among them, well-known actors of the FGF family or serum-responsive genes such as methylenetetrahydrofolate dehydrogenase (*mthFd2*) (36), progressive ankylosis (*ank*) (19), RAB5C (*Rac3*) (21), and immediate-early response 3 (*Ier3*) (8) have been identified. Interestingly, we demonstrated modulation of FGF receptors 1 (upregulation) and 4 (downregulation) and downregulation of *Igfbp2*. These results corroborate the proliferative phenotype of the C2C12 cells and their dedifferentiation in the presence of FGF6, which has been previously reported (38), and show that *Igfbp2* may be implicated in the differentiation process in C2C12 cells in response to FGF6. Thus the product of *Igfbp2* is a well-known inhibitor of IGF-1. Some reports of the role of the IGF growth factor suggest its implication in the regulation of skeletal muscle adaptation in response to different phenotypic events

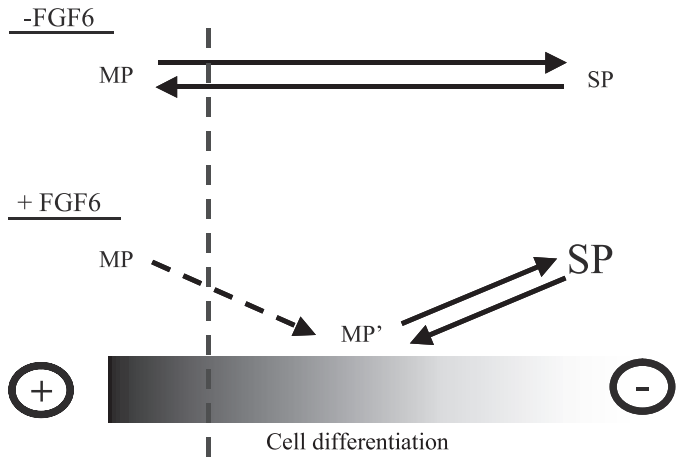


Fig. 6. Phenotypic and quantitative schematic evolution of the main population (MP) and SP cells in the presence or absence of FGF6. MP′, dedifferentiated population.

such as satellite cell proliferation and differentiation (42, 47), inhibition of apoptosis (30, 34), and improvement of the overall functional properties of skeletal muscles in dystrophic mice (4, 31). This suggests a potential role of FGF6 in the IGF pathway through the modulation of the expression of *Igfbp2*, and we hypothesize that this regulation may be preferentially involved in subpopulations of muscular SP cells. In addition, we observed a drift of the molecular program of the C2C12 cells that corroborates important modifications of C2C12 behavior in the presence of FGF6. These modifications concern the extracellular matrix and cytoskeleton structure with a downregulation of the transcription of major actors in their organization, such as procollagen, titin, and actin. The drift of the molecular program in C2C12 cells ends in a dedifferentiated phenotype that contributes to the increase of the SP cell population. This is confirmed by the upregulation of two well-known SC/SP cell markers, *Sca1* and CD34, and two molecular markers of dedifferentiation, *MDM2* and *Alcam*. Indeed, we found that *MDM2* is one of the most overexpressed genes in the presence of FGF. The protein encoded by this gene is known to inhibit MyoD function and muscular differentiation (15) and to induce $G_1$/S arrest (for a review, see Ref. 11). On the other hand, ALCAM (or CD166) is involved in homophilic adhesion as well as binding to CD6. Recently, the human homolog of ALCAM, hematopoietic cell antigen (HCA), was isolated by Cortes et al. (10), and this protein was detected in the most primitive subset of hematopoietic SCs as well as in myeloid progenitors in bone marrow. Here, we support this conjecture by demonstrating the upregulation of ALCAM in early progenitor muscular cells. These findings imply that ALCAM might be a key adhesion molecule involved in the characterization of SCs.

Finally, it appears that C2C12-derived SP cells probably correspond to a more immature cell population compared with the MP cells, thus confirming our previous reports indicating that the C2C12 cell line displays spontaneous cell heterogeneity, although it was initially clonal (5). We show that FGF6 increases the SP fraction in the C2C12 cell line and that M6 cells were different from parental MP (M2) cells, whereas S6 cells were similar to the original SP (S2). Thus a key question remains: whether the resulting S6 population derived from the accumulation of dedifferentiated MP cells in the presence of FGF6 or from direct mobilization of the resident SP subset. In previous reports, we showed that the SP derived from C2C12 cells was predominantly in the $G_0/G_1$ phase (5) and that the presence of FGF6 did not modify this state (23). These results suggested that the increase in the SP fraction in the C2CF6 cells was due to dedifferentiation and not to SP cell proliferation. Dye efflux in SP cells is mediated by membrane-associated P-glycoproteins of the ATP-binding cassette transporter family that act as energy-dependent pumps. Previous reports had shown that these proteins were associated with an increase in the population of cells with an immature phenotype (5, 9, 41, 52). Here, we identified two members of the ATP-binding cassette transporter family upregulated in presence of FGF6. It is predictable that many ATP-binding cassette transporters might show comparable effects provided their biological activities resulted in fashioning a similar metabolic environment by pumping out substrates and factors involved in sustaining cell differentiation. Here, we add support to this notion by showing that the increase of C2CF6-derived SP cells was due to the dedifferentiation of MP into M6 and S6 cells. The molecular mechanism involved in this process is still unknown, and we propose that the pumps implicated in the dye efflux in SP cells could be involved in this phenomenon. In conclusion, we hypothesize, as described in Fig. 6, that FGF6 triggers dedifferentiation of the C2C12 MP into a dedifferentiated population MP′ (M6), which is phenotypically different from the original cell population and has the capacity to "give rise" to SP cells (S6) similar to native C2C12 SP cells (S2). This finding suggests that the SC or immature phenotype of the SP subset of cells could be acquired by dedifferentiation of a main population of cells in adult tissues under environmental influence.

This provides a novel alternative for the maintenance or production of the SC population in addition to the classical self-renewal process.

## ACKNOWLEDGMENTS

The authors are grateful to Dr. Claude Dechesne (UMR6543-Centre National de la Recherche Scientifique, Nice, France) for providing the mouse and rat subtracted cDNA libraries. We also thank Terry Partridge, Vincent Frouin, and Carlo Lucchesi for many helpful discussions and Sophie Lemoine for technical support.

## GRANTS

The research carried out in the laboratory of the authors was supported by grants from the Association Française contre les Myopathies, the Commissariat à l'Energie Atomique, and the Centre National de la Recherche Scientifique.

## REFERENCES

1. **Alison MR, Poulsom R, Jeffery R, Dhillon AP, Quaglia A, Jacob J, Novelli M, Prentice G, Williamson J, and Wright NA.** Hepatocytes from non-hepatic adult stem cells. *Nature* 406: 257, 2000.
2. **Asakura A and Rudnicki MA.** Side population cells from diverse adult tissues are capable of in vitro hematopoietic differentiation. *Exp Hematol* 30: 1339–1345, 2002.
3. **Asakura A, Seale P, Girgis-Gabardo A, and Rudnicki MA.** Myogenic specification of side population cells in skeletal muscle. *J Cell Biol* 159: 123–134, 2002.
4. **Barton ER, Morris L, Musaro A, Rosenthal N, and Sweeney HL.** Muscle-specific expression of insulin-like growth factor I counters muscle decline in mdx mice. *J Cell Biol* 157: 137–148, 2002.
5. **Benchaouir R, Rameau P, Decraene C, Dreyfus P, Israeli D, Pietu G, Danos O, and Garcia L.** Evidence for a resident subset of cells with SP phenotype in the C2C12 myogenic line: a tool to explore muscle stem cell biology. *Exp Cell Res* 294: 254–268, 2004.
6. **Blau HM, Webster C, Chiu CP, Guttman S, and Chandler F.** Differentiation properties of pure populations of human dystrophic muscle cells. *Exp Cell Res* 144: 495–503, 1983.
7. **Bunting KD.** ABC transporters as phenotypic markers and functional regulators of stem cells. *Stem Cells* 20: 11–20, 2002.
8. **Charles CH, Yoon JK, Simske JS, and Lau LF.** Genomic structure, cDNA sequence, and expression of gly96, a growth factor-inducible immediate-early gene encoding a short-lived glycosylated protein. *Oncogene* 8: 797–801, 1993.
9. **Chaudhary PM and Roninson IB.** Expression and activity of P-glycoprotein, a multidrug efflux pump, in human hematopoietic stem cells. *Cell* 66: 85–94, 1991.
10. **Cortes F, Deschaseaux F, Uchida N, Labastie MC, Friera AM, He D, Charbord P, and Peault B.** HCA, an immunoglobulin-like adhesion molecule present on the earliest human hematopoietic precursor cells, is also expressed by stromal cells in blood-forming tissues. *Blood* 93: 826–837, 1999.
11. **Deb SP.** Function and dysfunction of the human oncoprotein MDM2. *Front Biosci* 7: d235–d243, 2002.
12. **Dudoit S and Fridlyand J.** A prediction-based resampling method for estimating the number of clusters in a dataset. *Genome Biol* 3: RESEARCH0036, 2002.

13. **Eglitis MA and Mezey E.** Hematopoietic cells differentiate into both microglia and macroglia in the brains of adult mice. *Proc Natl Acad Sci USA* 94: 4080–4085, 1997.
14. **Ferrari G, Cusella-De Angelis G, Coletta M, Paolucci E, Stornaiuolo A, Cossu G, and Mavilio F.** Muscle regeneration by bone marrow-derived myogenic progenitors. *Science* 279: 1528–1530, 1998.
15. **Fiddler TA, Smith L, Tapscott SJ, and Thayer MJ.** Amplification of MDM2 inhibits MyoD-mediated myogenesis. *Mol Cell Biol* 16: 5048–5057, 1996.
16. **Floss T, Arnold HH, and Braun T.** A role for FGF-6 in skeletal muscle regeneration. *Genes Dev* 11: 2040–2051, 1997.
17. **Goodell MA, Brose K, Paradis G, Conner AS, and Mulligan RC.** Isolation and functional properties of murine hematopoietic stem cells that are replicating in vivo. *J Exp Med* 183: 1797–1806, 1996.
18. **Goodell MA, Rosenzweig M, Kim H, Marks DF, DeMaria M, Paradis G, Grupp SA, Sieff CA, Mulligan RC, and Johnson RP.** Dye efflux studies suggest that hematopoietic stem cells expressing low or undetectable levels of CD34 antigen exist in multiple species. *Nat Med* 3: 1337–1345, 1997.
19. **Guo Y, Hsu DK, Feng SL, Richards CM, and Winkles JA.** Polypeptide growth factors and phorbol ester induce progressive ankylosis (ank) gene expression in murine and human fibroblasts. *J Cell Biochem* 84: 27–38, 2001.
20. **Gussoni E, Soneoka Y, Strickland CD, Buzney EA, Khan MK, Flint AF, Kunkel LM, and Mulligan RC.** Dystrophin expression in the mdx mouse restored by stem cell transplantation. *Nature* 401: 390–394, 1999.
21. **Haataja L, Groffen J, and Heisterkamp N.** Characterization of RAC3, a novel member of the Rho family. *J Biol Chem* 272: 20384–20388, 1997.
22. **Ihaka R and Gentleman R.** R: a language for data analysis and graphics. *J Comp Graph Stat* 5: 299–31423, 1996.
23. **sraeli D, Benchaouir D, Ziaei S, Rameau P, Gruszczynski C, Peltekian E, Danos O, and Garcia L.** FGF6 mediated expansion of a resident subset of cells with SP phenotype in the C2C12 myogenic line. *J Cell Physiol* 201: 409–19, 2004.
24. **Ivanova NB, Dimos JT, Schaniel C, Hackney JA, Moore KA, and Lemischka IR.** A stem cell molecular signature. *Science* 298: 601–604, 2002.
25. **Jackson KA, Majka SM, Wang H, Pocius J, Hartley CJ, Majesky MW, Entman ML, Michael LH, Hirschi KK, and Goodell MA.** Regeneration of ischemic cardiac muscle and vascular endothelium by adult stem cells. *J Clin Invest* 107: 1395–1402, 2001.
26. **Jackson KA, Mi T, and Goodell MA.** Hematopoietic potential of stem cells isolated from murine skeletal muscle. *Proc Natl Acad Sci USA* 96: 14482–14486, 1999.
27. **Kawada H and Ogawa M.** Bone marrow origin of hematopoietic progenitors and stem cells in murine muscle. *Blood* 98: 2008–2013, 2001.
28. **Kerr MK, Martin M, and Churchill GA.** Analysis of variance for gene expression microarray data. *J Comput Biol* 7: 819–837, 2000.
29. **Kondo T, Setoguchi T, and Taga T.** Persistence of a small subpopulation of cancer stem-like cells in the C6 glioma cell line. *Proc Natl Acad Sci USA* 101: 781–786, 2004.
30. **Leri A, Liu Y, Claudio PP, Kajstura J, Wang X, Wang S, Kang P, Malhotra A, and Anversa P.** Insulin-like growth factor-1 induces Mdm2 and down-regulates p53, attenuating the myocyte renin-angiotensin system and stretch-mediated apoptosis. *Am J Pathol* 154: 567–580, 1999.
31. **Lynch GS, Cuffe SA, Plant DR, and Gregorevic P.** IGF-I treatment improves the functional properties of fast- and slow-twitch skeletal muscles from dystrophic mice. *Neuromuscul Disord* 11: 260–268, 2001.
32. **McKinney-Freeman SL, Jackson KA, Camargo FD, Ferrari G, Mavilio F, and Goodell MA.** Muscle-derived hematopoietic stem cells are hematopoietic in origin. *Proc Natl Acad Sci USA* 99: 1341–1346, 2002.
33. **Mezey E and Chandross KJ.** Bone marrow: a possible alternative source of cells in the adult nervous system. *Eur J Pharmacol* 405: 297–302, 2000.
34. **Napier JR, Thomas MF, Sharma M, Hodgkinson SC, and Bass JJ.** Insulin-like growth factor-I protects myoblasts from apoptosis but requires other factors to stimulate proliferation. *J Endocrinol* 163: 63–68, 1999.
35. **Orkin SH and Zon LI.** Hematopoiesis and stem cells: plasticity versus developmental heterogeneity. *Nat Immun* 3: 323–328, 2002.
36. **Peri KG and MacKenzie RE.** $NAD^+$-dependent methylenetetrahydrofolate dehydrogenase-cyclohydrolase: detection of the mRNA in normal murine tissues and transcriptional regulation of the gene in cell lines. *Biochim Biophys Acta* 1171: 281–287, 1993.
37. **Pfaffl MW.** A new mathematical model for relative quantification in real-time RT- PCR. *Nucleic Acids Res* 29: E45–E45, 2001.
38. **Pizette S, Coulier F, Birnbaum D, and DeLapeyriere O.** FGF6 modulates the expression of fibroblast growth factor receptors and myogenic genes in muscle cells. *Exp Cell Res* 224: 143–151, 1996.
39. **Polesskaya A, Seale P, and Rudnicki MA.** Wnt signaling induces the myogenic specification of resident CD45+ adult stem cells during muscle regeneration. *Cell* 113: 841–852, 2003.
40. **Poulsom R, Alison MR, Forbes SJ, and Wright NA.** Adult stem cell plasticity. *J Pathol* 197: 441–456, 2002.
41. **Ramalho-Santos M, Yoon S, Matsuzaki Y, Mulligan RC, and Melton DA.** "Stemness": transcriptional profiling of embryonic and adult stem cells. *Science* 298: 597–600, 2002.
42. **Rosenthal SM and Cheng ZQ.** Opposing early and late effects of insulin-like growth factor I on differentiation and the cell cycle regulatory retinoblastoma protein in skeletal myoblasts. *Proc Natl Acad Sci USA* 92: 10307–10311, 1995.
43. **Sekowska A, Robin S, Daudin JJ, Henaut A, and Danchin A.** Extracting biological information from DNA arrays: an unexpected link between arginine and methionine metabolism in *Bacillus subtilis*. *Genome Biol* 2: RESEARCH0019, 2001.
44. **Takakura N, Watanabe T, Suenobu S, Yamada Y, Noda T, Ito Y, Satake M, and Suda T.** A role for hematopoietic stem cells in promoting angiogenesis. *Cell* 102: 199–209, 2000.
45. **Theise ND, Nimmakayalu M, Gardner R, Illei PB, Morgan G, Teperman L, Henegariu O, and Krause DS.** Liver from bone marrow in humans. *Hepatology* 32: 11–16, 2000.
46. **Uchida N, Fujisaki T, Eaves AC, and Eaves CJ.** Transplantable hematopoietic stem cells in human fetal liver have a $CD34^+$ side population (SP) phenotype. *J Clin Invest* 108: 1071–1077, 2001.
47. **Valentinis B and Baserga R.** IGF-I receptor signalling in transformation and differentiation. *Mol Pathol* 54: 133–137, 2001.
48. **Van Gelder RN, von Zastrow ME, Yool A, Dement WC, Barchas JD, and Eberwine JH.** Amplified RNA synthesized from limited quantities of heterogeneous cDNA. *Proc Natl Acad Sci USA* 87: 1663–1667, 1996.
49. **Wang X, Willenbring H, Akkari Y, Torimaru Y, Foster M, Al-Dhalimy M, Lagasse E, Finegold M, Olson S, and Grompe M.** Cell fusion is the principal source of bone-marrow-derived hepatocytes. *Nature* 422: 897–901, 2003.
50. **Yaffe D and Saxel O.** Serial passaging and differentiation of myogenic cells isolated from dystrophic mouse muscle. *Nature* 270: 725–727, 1977.
51. **Yang YH, Dudoit S, Luu P, Lin DM, Peng V, Ngai J, and Speed TP.** Normalization for cDNA microarray data: a robust composite method addressing single and multiple slide systematic variation. *Nucleic Acids Res* 30: e15, 2002.
52. **Zhou S, Schuetz JD, Bunting KD, Colapietro AM, Sampath J, Morris JJ, Lagutina I, Grosveld GC, Osawa M, Nakauchi H, and Sorrentino BP.** The ABC transporter Bcrp1/ABCG2 is expressed in a wide variety of stem cells and is a molecular determinant of the side-population phenotype. *Nat Med* 7: 1028–1034, 2001.